

Cite this: *J. Mater. Chem. B*, 2023,  
11, 6265

## Supramolecular assemblies of multifunctional microgels for biomedical applications

Jingxia Zheng,<sup>a</sup> Canjie Zhu,<sup>a</sup> Xun Xu,<sup>b</sup> Xinwei Wang<sup>b</sup> and Jun Fu \*<sup>a</sup>

Biomedical materials with outstanding biochemical and mechanical properties have great potential in tissue engineering, drug delivery, antibacterial, and implantable devices. Hydrogels have emerged as a most promising family of biomedical materials because of their high water content, low modulus, biomimetic network structures, and versatile biofunctionalities. It is critical to design and synthesize biomimetic and biofunctional hydrogels to meet demands of biomedical applications. Moreover, fabrication of hydrogel-based biomedical devices and scaffolds remains a great challenge, largely due to the poor processibility of the crosslinked networks. Supramolecular microgels have emerged as building blocks for fabrication of biofunctional materials for biomedical applications due to their excellent characteristics, including softness, micron size, high porosity, heterogeneity and degradability. Moreover, microgels can serve as vehicles to carry drugs, bio-factors, and even cells to augment the bio-functionalities to support or regulate cell growth and tissue regeneration. This review article summarizes the fabrication and the mechanism of supramolecular assemblies of microgels, and explores their application in 3D printing, along with detailed representative biomedical applications of microgel assemblies in cell culture, drug delivery, antibacterial and tissue engineering. Major challenges and perspectives of supramolecular microgel assemblies are presented to indicate future research directions.

Received 17th February 2023,  
Accepted 18th May 2023

DOI: 10.1039/d3tb00346a

rsc.li/materials-b

### 10th anniversary statement

Congratulations on the 10th anniversary of the *Journal of Materials Chemistry* family. I am grateful to have had twenty papers published in *Journal of Materials Chemistry B* covering topics from implantable polymers, tough hydrogels, tissue engineering scaffolds, soft actuators, and hydrogel-based flexible electronics. All these research articles and reviews have been well acknowledged by readers, thanks to the outstanding efforts by the editorial team and the volunteer referees. I am honored to have served as an Advisory Board Member since 2017. It provides me with great opportunities to make more contributions to this journal and the community. This review article introduces an emerging field of microgel-based 3D printing for biomedical materials. This important concept proposes to utilize microgels as functional building blocks to construct multifunctional and high performance biomedical devices. Supramolecular chemistry plays critical roles in spontaneously and efficiently assembling microgels together. This supramolecular strategy can be readily applied to integrate microgels loaded with drugs, factors, peptides, enzymes, and even cells into soft chips, organoids, and artificial biotissues. I hope this review will be of broad interest to readers in the field of biomedical materials and engineering.

## 1. Introduction

Biomaterials play an extremely important role in biomedical engineering through integration and interactions with other functional substances such as cells, growth factors, drugs and genes.<sup>1</sup>

<sup>a</sup> Key Laboratory of Polymeric Composite and Functional Materials of Ministry of Education, Guangdong Functional Biomaterials Engineering Technology Research Centre, Guangzhou Key Laboratory of Flexible Electronic Materials and Wearable Devices, School of Materials Science and Engineering, Sun Yat-sen University, Guangzhou Higher Education Mega Centre, 132 Waihuan Road East, Panyu, Guangzhou 510006, China. E-mail: fujun8@mail.sysu.edu.cn

<sup>b</sup> State Key Laboratory of Polyolefins and Catalysis, Shanghai Research Institute of Chemical Industry, Shanghai 200062, China

Biocomposites can be used as a 3D matrix for cell or drug delivery, by protecting them from unwanted mechanical damage.<sup>2</sup> Moreover, biomaterials with optimal biochemical and mechanical properties can promote cell survival and retention, and promote cell-mediated tissue matrix production and vascularization,<sup>3</sup> which has been widely used to promote cell delivery and tissue regeneration.<sup>4,5</sup> Supramolecular assembly is prevalent in biomedical systems that organize biomacromolecules into hierarchical structures and biotissues.<sup>6,7</sup> The generation of supramolecular materials assembled by transient cross-linking facilitates engineering of multifunctional, self-assembled, stimuli-responsive biomaterials.<sup>8</sup>

Hydrogels have broad application prospects as biomaterials due to the high water content, adjustable physicochemical

properties and structural similarity to the natural extracellular matrix (ECM).<sup>9</sup> However, the tight nanometer-scale cross-linking network of traditional block hydrogels is unfavorable for the penetration of cells and blood vessels, and it is hard to process or damage the biological activity and endogenous healing performance during extruding. To tackle this problem, many types of hydrogels have been processed into microgels *via* a variety of fabrication techniques,<sup>10</sup> including mechanical crushing,<sup>11–13</sup> emulsion polymerization,<sup>14–17</sup> microfluidic and microchannel,<sup>18–21</sup> and templating methods.<sup>22–24</sup> By using various assembly principles including jamming,<sup>25–27</sup> chemical bonding,<sup>28–30</sup> or non-covalent interactions,<sup>31–33</sup> microgels have been processed into assemblies with many excellent characteristics, including softness, micron size, high porosity, heterogeneity and degradability.<sup>9,34</sup>

Supramolecular microgels are made of a variety of materials, which mainly include host–guest molecules such as cyclodextrin, Cucurbit[8]uril, adamantane, azobenzene, and ferrocene,

synthetic polymers such as polyethylene glycol (PEG), poly-(*N*-isopropyl acrylamide) (PNIPAAm), and natural polysaccharides, like hyaluronic acid, sodium alginate, *etc.* The structures of supramolecular microgel assemblies determine multifunctional performance and biomedical applications. Supramolecular microgel assemblies are cross-linked by non-covalent interactions, which are weak and dynamic, and result in beneficial properties, including self-healing, shear thinning, injectability, or printability.<sup>12,30,35</sup> The micron size of microgels allows for minimal invasive injection. Most microgels are amiable to protect cells during injection and transportation, and are ideal candidates for 3D printing bioinks to fabricate artificial tissues and organs. Therein, collective dynamic supramolecular interactions help maintain the stability of printed scaffolds. Moreover, microgels with different formulations like materials, composition, size and contents can be used as modules to create multifunctional materials and constructs. Microgel scaffolds are usually porous, which is conducive to cell invasion, proliferation and migration.<sup>36,37</sup>



**Jingxia Zheng**

*Jingxia Zheng obtained her bachelor's degree in materials chemistry from School of Materials Science and Engineering, Sun Yat-sen University in 2021. She is currently pursuing a Masters degree supervised by Prof. Jun Fu at School of Materials Science and Engineering, Sun Yat-sen University. Her research interests include functional hydrogels for 3D printing flexible electronics.*



**Canjie Zhu**

*Canjie Zhu graduated from the School of Chemical Engineering and Technology of Sun Yat-sen University with a bachelor's degree in chemical engineering and technology in 2022. Now he is pursuing a Masters degree supervised by Prof. Jun Fu at School of Materials Science and Engineering, Sun Yat-sen University. His research interests include functional hydrogels for flexible electronics.*



**Xun Xu**

*Xun Xu, Master of Science, graduated from the Department of Chemical and Materials Engineering, New Mexico State University in 2015. He is working at the State Key Laboratory of Polyolefins and Catalysis Materials, Shanghai Research Institute of Chemical Industry Co., Ltd. He is now focusing on the fabrication and modification of polyolefin biomaterials, including artificial joints, ligaments, etc.*



**Xinwei Wang**

*Dr Xinwei Wang is a professor-level senior engineer working at the State Key Laboratory of Polyolefins and Catalysis Materials, Shanghai Research Institute of Chemical Industry Co., Ltd (SRICI). He obtained his bachelor's degree from Taiyuan University of Technology in 2000, Master's degree from Donghua University in 2003, and PhD in material science and engineering from Donghua University in 2007. He worked at PGI Nonwovens (China) Co., Ltd. as an R&D supervisor for 1 year and moved to SRICI in 2008. His research focuses on catalytic polymerization, processing, modification, and characterization of ultra-high molecular weight polyethylene materials.*

What's more, multi-stimuli responsiveness is another important feature of supramolecular microgel assemblies, which respond to a variety of physical or biochemical stimuli<sup>38–40</sup> like temperature, light, magnetic/electric field, mechanical force, pH, and redox, *etc.* Responsive microgels serve as intelligent carriers for bioactive molecules such as drugs, proteins, carbohydrates and DNA. Based on the micro porous structures and multifunctional characteristics of supramolecular microgel assemblies, they are suitable for broad biomedical applications, including cell transplantation,<sup>41</sup> drug delivery,<sup>42–44</sup> antibacterials,<sup>45</sup> biocatalysis,<sup>46</sup> and tissue engineering,<sup>34,36</sup> *etc.*

In this review article, we discuss the latest advances of supramolecular assemblies of multifunctional microgels for biomedical applications. Firstly, we simply introduce the fabrication of microgels. Next, we introduce the mechanism of supramolecular assemblies of microgels, including host-guest interactions, hydrogen bonding, metal coordination and electrostatic interaction, *etc.* Then, we briefly describe 3D printing of supramolecular microgels, and summarize in detail representative applications of microgel assemblies in cell culture, drug delivery, antibacterial and tissue engineering. Finally, we present the major challenges and perspectives of supramolecular microgel assemblies to indicate future research directions (Fig. 1).

## 2. Fabrication of microgels

A variety of fabrication techniques of microgels have been developed,<sup>10</sup> including mechanical crushing, emulsion polymerization, microfluidic/microchannels and templating<sup>47</sup> (Fig. 2). In general, these methods involve particle formation and gelation. Particles are prepared by dispersing an aqueous monomer solution droplet in organic solution. Then, the



Jun Fu

*Dr Jun Fu is a Professor at the School of Materials Science and Engineering at Sun Yat-sen University (SYSU). He obtained his BSc in applied chemistry at Wuhan University in 1999, and a PhD in polymer chemistry and physics from Changchun Institute of Applied Chemistry, Chinese Academy of Sciences (CAS) in 2005. He was a visiting scholar at Max Planck Institute for Polymer Research from 2005 to 2007, and a research fellow at*

*Massachusetts General Hospital/Harvard Medical School from 2007 to 2010. He was appointed as a professor at Ningbo Institute of Materials Technology and Engineering, CAS, in 2010, and then moved to SYSU in 2019. His research focuses on high performance and functional hydrogels for biomimetic, wearable and implantable devices.*



Fig. 1 Supramolecular microgel assemblies and applications.

monomers in particles are initiated to polymerize and crosslink by heating or irradiation to form microgels with 100 nm–1 mm diameters.<sup>48,49</sup> This section briefly outlines representative microgel preparation methods.

### 2.1 Mechanical crushing

Microgels can be produced by mechanically breaking a pre-formed bulk hydrogel into microparticles (Fig. 2a).<sup>47</sup> For example, Sinclair *et al.* produced zwitterionic microgels by extruding bulk gels through progressively fine steel meshes using a stainless-steel piston and cylinder apparatus. The microgels were sieved for at least three times to obtain diameters of 15–30  $\mu\text{m}$ .<sup>11</sup> Moreover, Fu *et al.* extruded crosslinked chitosan methacrylate (CHMA)/polyvinyl alcohol (PVA) hydrogels through nozzles repeatedly with specific internal diameters from 300 to 500  $\mu\text{m}$  to produce a slurry of microparticles with an average diameter of  $197 \pm 68 \mu\text{m}$ .<sup>12</sup> Hinton *et al.* used a rotational blender to break a crosslinked gelatin hydrogel into microgels with diameters of 120–300  $\mu\text{m}$ ,<sup>13</sup> which can be used as ink for 3D printing various structures into a supporting bath. These mechanical crushing methods are high-speed, simple and suitable for various materials; however, the particle sizes are usually polydisperse.

### 2.2 Emulsion polymerization

Many methods based on emulsion polymerization have been reported to prepare microgels, mainly including surfactant-free emulsion polymerization and emulsion polymerization with added surfactant (Fig. 2b).

Surfactant-free emulsion polymerization (SFEP) means that no surfactant is added at all or only a small amount of surfactant is added in the reaction process (with a concentration lower than the critical micelle concentration CMC),



Fig. 2 Fabrication techniques of microgels, including (a) mechanical crushing, (b) emulsion polymerization, (c) microfluidic and microchannel and (d) templating methods. Reproduced with permission from ref. 47. Copyright 2019 Springer Nature.

which usually applies for thermosensitive monomers, typically with a lower critical solution temperature (LCST).<sup>50</sup> Such monomers are fully dissolved in water below the LCST to form a homogeneous system, and undergo phase separation to form droplets above the LCST. Therein, polymerization and crosslinking take place to yield microgels with collapsed configurations. Xue *et al.* prepared different microgels with narrow size distribution by SFEP of six acrylamide-type thermoresponsive monomers through free radical copolymerization.<sup>15</sup> However, SFEP is applicable to only a few thermosensitive monomers.

Emulsion polymerization with added surfactant includes conventional emulsion polymerization and inverse emulsion polymerization, which can form oil-in-water or water-in-oil emulsion by high-speed dispersing different monomers in the oil phase or water phase, respectively. Then, polymer microgels are formed by thermal initiation or photoinitiation before purification centrifugal washing. A homogeneous emulsification method, speed and time will affect the size and dispersity of microgels.<sup>51</sup> Inverse emulsion polymerization has the advantages of simplicity, rapidity and small particle size, and is suitable for the synthesis of various water-soluble microgels, including poly(2-acrylamido-2-methyl-propanesulfonic acid) (PAMPS), poly-acrylamide (PAAm), poly-acrylic acid (PAAc), poly(*N*-isopropylacrylamide) (PNIPAm), poly(2-hydroxyethyl methacrylate) (PHEMA), poly(ethylene glycol) (PEG), *etc.*, as well as biocompatible and degradable polysaccharide-based hybrid microgels like gelatin, alginate, chitosan, hyaluronic acid cellulose, *etc.*<sup>16,17</sup>

### 2.3 Microfluidic and microchannels

Microfluidic and microchannel techniques have been widely used to continuously prepare microgels with uniform and controllable particle compositions, dimensions, shapes, and pore sizes by altering flow rates and channel properties like

diameters, shapes, polarity, and architecture.<sup>52–54</sup> Common microchannel structures are T-shaped and  $\psi$ -shaped (Fig. 2c). Generally, the hydrogel precursor solution is injected into the oil phase to form spherical particles through a narrow channel due to interfacial tension, and then the environmental conditions are changed to crosslink the particles into microgels with diameters ranging from around 100 nm to 1000  $\mu\text{m}$ .<sup>55</sup> The microgels usually have excellent monodispersity.<sup>56</sup> Xu *et al.* used a flow-focusing V-shaped microfluidic chip with two water phase channels and one oil phase channel manufactured by soft lithography to prepare cross-linked gelatin microgels with enzymes.<sup>18</sup> A method to control the spatial distribution of structural proteins in microgels under mild gelation conditions by controlling the mixing of gelatin and physical and enzymatic cross-linking through microfluidics was demonstrated.

In addition, the microfluidic droplet generator can be used to generate highly uniform microgel building blocks, manufacture controlled interconnected microporous scaffolds, promote cell proliferation and network, and accelerate wound healing.<sup>57–59</sup> For example, Di Carlo *et al.* described a method for manufacturing highly uniform microgel building blocks in a continuous, scalable, high-throughput manner, so as to form a highly modular microporous environment for cell and tissue growth.<sup>19</sup> Hydrogel precursors are injected into the parallel step emulsification microfluidic device at a reduced nonreactive pH to generate uniform spherical microgel templates. Then, a unique pH adjustment was used to induce controllable and uniform crosslinking of microgel building blocks, and the productivity was one to two orders of magnitude higher than that of similar projects.<sup>20,21</sup> These controllable and degradable microgels fabricated by microfluidic and microchannel methods have the potential of non-uniform or gradient reactors, which can be used for 3D cell culture scaffolds and as components of complex and natural-inspired robots.

## 2.4 Templating

It is convenient to use templates to form particles of various sizes for crosslinking to form microgels triggered by environmental stimulation.<sup>22–24</sup> Among these, the photolithography process of hydrogel templating in a highly controllable and repeatable manner has become an attractive “top-down” alternative to traditional microgel synthesis technologies,<sup>60</sup> because it meets the requirement of preparing microgels with highly controllable size and morphology. Photolithographic patterned microgels can be prepared by any routes commonly used to generate cross-linked polymer networks, including chemical cross-linking, physical association and molecular self-assembly.<sup>61</sup> Essentially, the photolithographic synthesis of microgels involves transferring pre-designed template patterns to hydrogel precursors, and then (or accompanying) polymerization and/or cross-linking, separating to form microgels.<sup>62</sup> Various emerging lithography technologies for the synthesis of complex microgels can be divided into three categories: imprint lithography, lithography and flow lithography (Fig. 2d). Doyle *et al.* demonstrated a simple method for preparing non spherical chitosan polyethylene glycol (PEG) microgels based on a photolithographic template method for coupling of high surface density biomolecules.<sup>22</sup> Wu *et al.* used a soft lithography technology to produce alginate microgels with a highly controllable shape and uniform size ranging from several microns to millimeters by changing the corresponding parameters in the soft lithography method.<sup>63</sup>

## 3. Supramolecular assembling of microgels

Supramolecular interactions between microgels, including guest–host recognition, hydrogen bonding, electrostatic attraction, metal–ligand coordination, can work alone or collectively to assemble microgels into aggregates, structured constructs, and even macroporous materials under mild ambient conditions. Supramolecular assembling of microgels is reversible and usually friendly to cells and tissues, which is beneficial to biomedical applications. By introducing supramolecular moieties into microgels, it is convenient to tune the ability to assemble microgels in

the desired manner into pre-designed microstructures. Besides, the assemblies exhibit shear thinning and self-healing, which is highly desired for injection, processing, and 3D printing. In this way, microgels with different components and functionalities can be assembled into multifunctional constructs. Specifically, microgels carrying different drugs or cells can assemble into single devices to achieve concerted therapy or regeneration. This section introduces recent progress in representative supramolecular assembling of microgels.

### 3.1 Host–guest recognition

Host–guest recognition usually refers to supramolecular interactions between molecules based on geometric fitting and non-covalent association (Fig. 3a).<sup>40</sup> Host molecules with cavities, including crown ethers, cyclodextrins, calixarenes, column aromatics and cucurbitacin, *etc.*, usually offer a tiny amount of room for a guest molecule to fit in. Therein, both the geometry recognition and hydrophobic/hydrophilic/coordination interactions work together to form a stable non-covalent associate. This is known as host–guest supramolecular recognition. The association constant for a host–guest pair is primarily determined by the hydrophilicity, size, polarity, and charge of the guest. Guests with different association constants may compete to occupy the host cavity. When the host or guest moieties are linked to polymer chains, numerous host–guest complexes can form to serve as non-covalent bonding and crosslinking, resulting in non-covalent crosslinks that are responsive to external stimuli (Fig. 3b).<sup>44</sup>

**Cyclodextrin.** Cyclodextrins are a family of cyclic oligosaccharides with repeating D-glucose units. CDs with 6, 7, or 8 saccharide cycles are known as  $\alpha$ -,  $\beta$ -, or  $\gamma$ -cyclodextrins with a hydrophobic cavity (Fig. 4a).<sup>64</sup> The CDs can combine with hydrophobic guests with molecular size fitting the cavity, such as a linear alkyl chain, adamantane (Ad), azobenzene (Azo), and ferrocene (Fc).<sup>65</sup> The cavity sizes of CDs are a little different, and in the host–guest complexation process, hydration water molecules in the CD cavities are partially replaced by hydrophobic guest molecules.<sup>66</sup> The association constant for Ad and  $\beta$ -CD, for example, is about  $10^4$ – $10^5$  M<sup>-1</sup>,<sup>67–69</sup> whereas that for Fc and  $\beta$ -CD is about  $10^2$ – $10^3$  M<sup>-1</sup>.<sup>70,71</sup> The spherical Ad group



Fig. 3 (a) Host–guest recognition. Reproduced with permission from ref. 40. Copyright 2022 John Wiley and Sons. (b) Different kinds of host–guest complexes. Reproduced with permission from ref. 44. Copyright 2021 Elsevier.

with a diameter of 7 Å can perfectly match the cavity diameter of  $\beta$ -CD.<sup>72</sup> This behavior has been utilized to trigger responsive changes of supramolecular hydrogels and microgels.<sup>73,74</sup>

Hydrogels with host and/or guest moieties can form assemblies through supramolecular recognition at the interface between dangling host or guest groups. Of particular interest is the supramolecular assembly of microgels as multifunctional building blocks into macroscopic constructs with biomimetic structures and functionalities for drug release, cell encapsulation, and tissue engineering. In order to synthesize microgels functionalized with host and/or guest groups, four-armed PEG is functionalized on the ends by using thiol click chemistry to bond either  $\beta$ -cyclodextrin or adamantane. Microgels separately synthesized from  $\beta$ -CD- or Ad-functionalized four-arm PEGs self-assemble through reversible guest–host interactions between microgel particles when mixed, generating an interlinked network (Fig. 4b).<sup>75</sup> Burdick *et al.* used a PDMS microfluidic device<sup>78</sup> to manufacture cross-linked hyaluronic acid (HA) microgels with covalent cross-linking in modular particles. The microgels modified with cyclodextrin and adamantane formed hydrogels through interparticle guest–host linking.<sup>20,79</sup> The two-component microgels show shear-thinning and self-healing, which makes it easy to inject into dynamic environments. The multiple material components and high porosity make the microgels suitable for cell delivery. Besides, methacrylate

modified  $\beta$ -cyclodextrin (host) and vinyl ferrocene (guest) formed redox cleavable crosslinkers through host–guest inclusion for the synthesis of microgels with variable content of redox cleavable crosslinkers through precipitation polymerization. The microgel assemblies were used for effective loading and release of anticancer drugs.<sup>80</sup>

Host–guest supramolecular assemblies are usually responsive to external stimuli, including light, temperature, and redox reactions,<sup>76,81–83</sup> primarily depending on the responsive properties of the guests. Such responsiveness is usually reversible and can be utilized for injection, advanced manufacturing, drug delivery, cell encapsulation and delivery, *etc.*

Self-assembly of soft colloids with light-switchable supramolecular interactions can be triggered to dissociate upon exposure to light. Azobenzene (Azo) functionalized nanogels (the guest colloid) and  $\alpha$ -cyclodextrin functionalized microgels (the host colloid) can form stable colloid clusters through supramolecular recognition between the Azo and  $\alpha$ -CD moieties dangling on the surfaces of the nanogels.<sup>81</sup> When exposed to UV light, the Azo groups experience a transition from *trans*-conformation to *cis*-conformation. Since the *cis*-Azo has a much lower association constant with  $\alpha$ -CD than that for *trans*-Azo/ $\alpha$ -CD,<sup>84,85</sup> the interface recognition becomes weaker, thus the colloidal clusters disassemble under UV light. Subsequently, when the solution is exposed to visible light, the colloids



Fig. 4 The host–guest recognition for CDs and CB[8]. (a) Schematic structures of  $\alpha$ -,  $\beta$ -, and  $\gamma$ -CD. Reproduced with permission from ref. 64. Copyright 2014 American Chemical Society. (b) A reversible host–guest interaction between microgel particles functionalized with Ad and  $\beta$ -CD. Reproduced with permission from ref. 75. Copyright 2021 The Royal Society of Chemistry. (c) Guest molecules ( $\beta$ -CD) and host molecules (Fc) for the construction of Fc-containing hydrogels. Reproduced with permission from ref. 76. Copyright 2020 Elsevier. (d) Supramolecular hydrogel fabrication through the host–guest interactions between the FGG-EA and CB[8]. Reproduced with permission from ref. 77. Copyright 2017 American Chemical Society. (e) Supramolecular assembly between HBPCB[8] and HEC-Np. Reproduced with permission from ref. 31. Copyright 2018 John Wiley and Sons.

re-assemble into clusters. The reversible colloidal self-assembly can be controlled by the interplay between the supramolecular and covalent crosslinking, and can also be adjusted by the addition of competitive host molecules. Han *et al.* incorporate supramolecular assembling and electrostatic interactions between microgels, and investigate the delicate balance between colloidal-range electrostatic repulsion and supramolecular-range host/guest driven attraction in  $\alpha$ -CD/azobenzene modified host/guest co-assembling microgel systems.<sup>86</sup> By labeling microgels with fluorescent moieties, the authors identified three different states of assembly (disassembled, dispersed co-assembled clusters, co-assembled flocculates). The kinetic balances between the multivalent and cooperative binding of the host/guest complexes and the electrostatic repulsion leads to trapped metastable configurations and reconfiguration into string-like assemblies.

Redox reactions can change the chemical structure and hydrophilicity of guest molecules, which trigger disassembly of host-guest microgels.<sup>76</sup> Ferrocene (Fc) is a famous guest molecule that complexes with  $\beta$ -CD through supramolecular recognition (Fig. 4c). Once ferrocene is oxidized into Fc ions, the complex decomposes. Microgels copolymerized from acrylic acid, ferrocene-modified *N*-(3-aminopropyl) methacrylamide and *N,N'*-methylenebisacrylamide (MBAA) are responsive to electrochemical oxidation of the ferrocene groups.<sup>82</sup> Such electrochemical responsive Fc-containing microgels may find applications as particle stabilizers for potential-stimulated Pickering emulsions. Microgels are synthesized from cyclodextrin functionalized 8-arm poly(ethylene glycol) (8A PEG-CD) and ferrocene modified counterparts (8A PEG-Fc) *via* CD/Fc host-guest chemistry to form Pickering emulsions. Taking advantage of the redox reaction of Fc, the formation and deformation of the microgels and corresponding Pickering emulsions can be reversibly triggered by external potential.<sup>83</sup> Poly(ionic liquid) (PIL) microgels modified with ferrocene (Fc) are electrochemically active and can respond reversibly to redox stimulus. Fc-Anchored PIL microgels are used as the building blocks for supramolecular self-assembly with a  $\beta$ -cyclodextrin ( $\beta$ -CD) dimer through host-guest inclusion complexation. The assembled PIL microgels could undergo reversible association and dissociation as triggered by electrochemical redox reaction.<sup>87</sup> Such supramolecular crosslinking on the basis of Fc- $\beta$ -CD host-guest interactions is cleavable.<sup>80</sup>

**Cucurbit[8]uril.** Cucurbit[*n*]uril belongs to the family of cycloroxanes, and is a kind of macrocyclic host molecule with a “pumpkin”-shaped symmetric barrel. As a “molecular container” of guest molecules, the host-guest binding process of CB[*n*]s involves the hydrophobic effect generated by the hydrophobic cavity, as well as the ion-dipole and hydrogen-bond interaction generated by the inlet of carbonyl-liner. Therefore, many neutral or positively charged objects can bind to CB[*n*]s with very high binding constants, which can yield supramolecular polymers.<sup>88</sup> Cucurbita[8]uridine (CB[8]) is unique and noteworthy in the Cucurbita[*n*]uridine family, because it has a relatively large cavity, so as to accommodate two guest molecules at the same time. The guest molecules combine with macrocyclic molecules to form discrete host-guest complexes.

The macrocyclic host molecules can act as catalysts, and combine with complexation induced  $pK_a$  shifts,<sup>89</sup> which can activate molecules, improve their bioavailability, and have great potential in drug delivery.<sup>90</sup> By combining polymer science and CB[8] host guest chemistry, a variety of systems have been established to construct supramolecular polymers, which usually exist in the form of polymer networks and hydrogels, microcapsules, micelles, vesicles and colloidal particles.<sup>91</sup>

Supramonomers assembled from reactive host and guest molecules have been developed for the synthesis of supramolecular microgels. Zhang *et al.*<sup>77</sup> devised and assembled tripeptide Phe-Gly-Gly/cucurbit[8]uril (CB[8]) host-guest supramonomers with one acrylate moiety on each end (Fig. 4d). Then the supramonomers were copolymerized with *N*-isopropylacrylamide (NIPAm) in aqueous solution to synthesize thermo-responsive supramolecular microgels. Moreover, the microgels exhibited stimuli-responsive and degradable properties benefiting from the dynamic nature of supramonomers.<sup>92</sup> Yu *et al.*<sup>31</sup> encapsulated two kinds of guests (viologen and naphthyl) in the cavity of macrocyclic host molecule CB[8] through molecular recognition to form a solid hetero-ternary host-guest supramolecular copolymer to prepare microgels (Fig. 4e).<sup>93,94</sup> The interaction between molecules is reversible, so the scaffolds formed by microgels are dynamically stable and self-healing. Inclusion complexes of alkyl pyridinium-containing acrylamide monomers with CB[8] facilitate supramolecular crosslinking in a series of hydrogels formed through *in situ* polymerization. The resulting hydrogels show greatly enhanced mechanical properties over a purely acrylamide-based gel. Moreover, by selecting fluorescent pyridine moieties, the materials exhibit fluorescence properties for sensing applications.<sup>95</sup>

### 3.2 Hydrogen bonding

Hydrogen bonding is prevalent between functional groups with electron donating and accepting capabilities. Ury, for example, is a group that is widely known to establish robust hydrogen bonding through three donor-acceptor pairs to form a dimer. Other functional groups like imidazole, amine, carboxylic acid, and OH groups are recognized as important elements for hydrogen bonding. Although a single hydrogen bond is weak, abundant hydrogen bonds between microgels can provide a high mechanical strength to microgel assemblies.<sup>96</sup> DNA base complementation and peptide self-assembly, as ubiquitous hydrogen bond interactions in organisms, have sequence specificity and high programmability, and can precisely regulate hydrogen bond interactions between microgels.<sup>97</sup> Qi *et al.* modified the DNA strands on the specified surfaces of PEGDA microgel cubes to produce an asymmetric glue pattern,<sup>33</sup> which induced the assembly of microgel cubes with different structures, such as linear chains, open networks, T-junctions and square structures in aqueous or interface systems (Fig. 5a). Microgels based on complementary nucleobase molecular recognition<sup>98</sup> were synthesized by polymerizing a series of bis-thymine end decorated flexible poly(*N*-isopropyl acrylamide) (T-PNIPAM-T) with a rigid poly[1-(4-vinyl benzyl)] adenine (PSA) (Fig. 5b). The nucleobase complementary pairing resulted in supramolecular cross-linked 3D



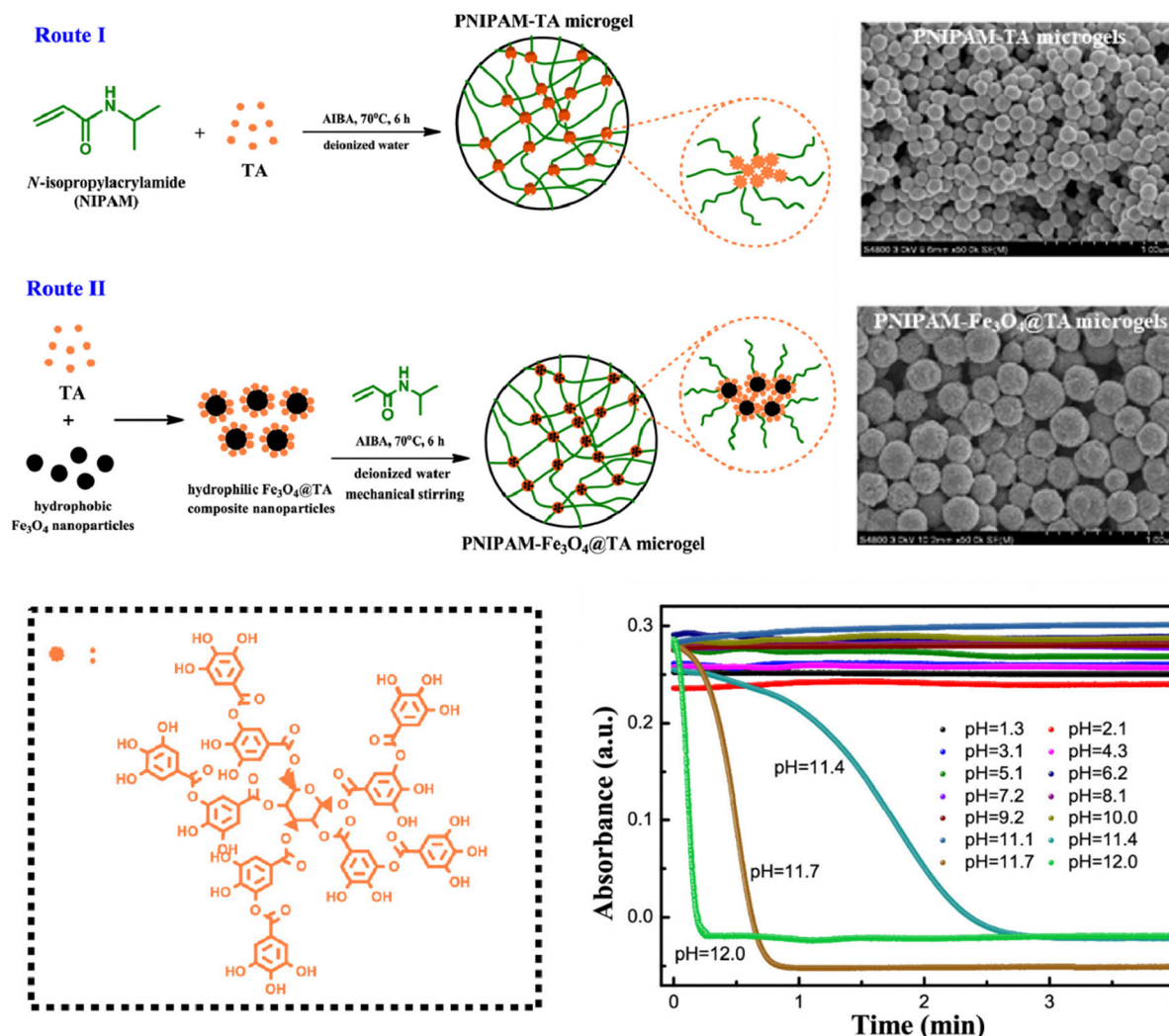


Fig. 6 PNIPAM-TA microgels fabricated *via* hydrogen bonding and the pH-dependent degradation. Reproduced with permission from ref. 102. Copyright 2019 American Chemical Society.

supramolecular iron(II)-bis-terpyridine coordination complexes between neighboring microgels provide sufficient strength and robustness of printed scaffolds to maintain integrity during applications for over two months.<sup>106</sup> The metallo-supramolecular assemblies are reversible (Fig. 7a). The [MIITPy<sub>2</sub>]<sup>2+</sup> complexes with metal cation (Fe(II) or Co(II)) as supramolecular links between microgels can break up upon oxidation and thus the connected microgels can disassemble into individual microgel building blocks (Fig. 7b).<sup>107</sup>

### 3.4 Electrostatic interaction

Microgels carrying negative or positive charges can self-assemble into clusters primarily driven by electrostatic attractions at the interface. Microgels can gain either negative charges or positive charges by using anionic or cationic monomers for the synthesis of microgels. Besides, microgels with chargeable functional groups in the network can gain charges in acidic or alkaline conditions. Electrostatic attractions are dynamic, reversible, and responsive to environmental conditions.

For example, changes in pH and/or ion strength in solution can significantly strengthen or block the electrostatic interactions between microgels, which induce assembling or disassembling of microgels.

Highly anisotropic supramolecular microtubules and soft spherical fluorescent microgels carrying charges self-assembled into various suprastructures. Microgels with positive and negative charges are synthesized by using polystyrene nanoparticles as seeds modified with cationic CTAB and anionic V50 respectively for polymerization with PNIPAM and PNIPMAM. These charged microgels self-assemble with supramolecular bile salt tubules with cationic or anionic charges to form hierarchical self-assembly into various superstructures varying from virus-like assemblies to supracolloidal networks.<sup>108</sup>

Zwitterionic moieties, comprised of equivalent negative and positive charges linked by a spacer of a few C-C bonds, can form strong ion-dipole and dipole-dipole interactions between polymer chains and microgels. Hydrogels formed from pure zwitterionic polycarboxybetaine (PCB) have been reported to

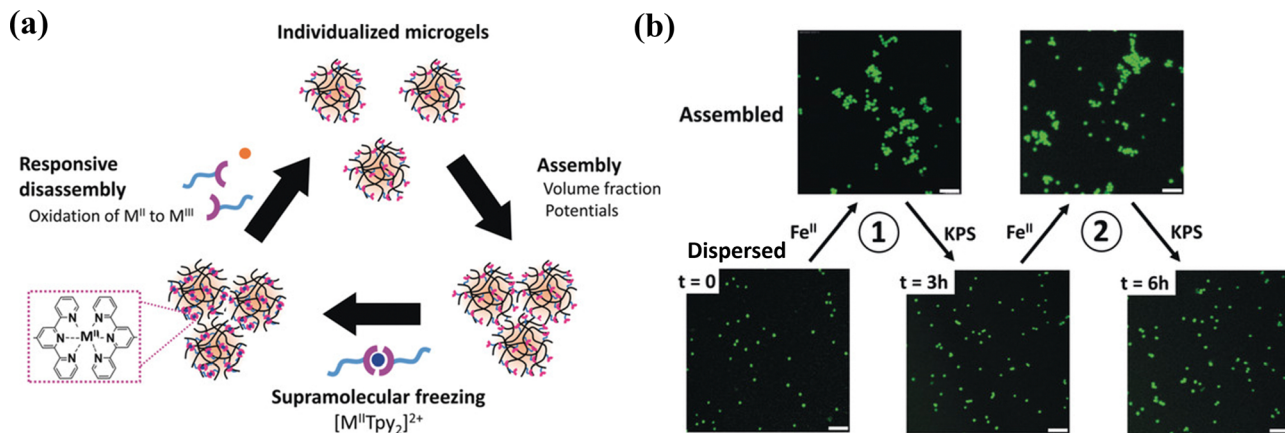


Fig. 7 Reversible metallo supramolecular assemblies of the  $[M^{II}(Tpy)_2]^{2+}$  complexes with metal cation ( $Fe^{II}$  or  $Co^{II}$ ). Scale bar: 5  $\mu m$ . Reproduced with permission from ref. 107. Copyright 2020 John Wiley and Sons.

inhibit the foreign body response and resist collagenous encapsulation *in vivo*,<sup>109</sup> and shield proteins from immunogenic responses.<sup>110</sup> Moreover, stem cells encapsulated in PCB hydrogels maintain their therapeutic multipotency and avoid nonspecific differentiation.<sup>111</sup> Zwitterionic microgels based on carboxybetaine acrylamide monomers are used as self-healing “building blocks” for injectable and malleable PCB hydrogel platform and cell-protective constructs (Fig. 8).<sup>112</sup> The microgels are beneficial to evade the foreign body reaction and preserve stem cell multipotency. The non-covalent interactions between microgels

enhance the overall self-healing associations (zwitterionic fusion) and increase construct elasticity, with an ideal modulus for cell culture and injection applications.

#### 4. 3D printing of supramolecular microgels

As an extremely important additive manufacturing method, 3D printing mainly includes extrusion bioprinting,<sup>113,114</sup> digital



Fig. 8 Injectable hydrogels formed by electrostatic and dipole interactions between zwitterionic microgels. Reproduced with permission from ref. 112. Copyright 2018 John Wiley and Sons.

light processing (DLP) printing<sup>115,116</sup> and inkjet printing.<sup>117,118</sup> Among these, extrusion 3D bioprinting usually relies on the rheological behaviours, shear thinning, and self-healing capability, and subsequent gelation of ink. Supramolecularly assembled microgels are linked through reversible non-covalent interactions and thus show necessary rheological behaviors for extrusion 3D printing. Such unique rheological properties allow for 3D printing under mild conditions, which are important for fabrication of cell-laden biological constructs. On the other hand, microgel assemblies are used as a supporting bath for 3D printing solutions of biomacromolecules like collagen into engineered scaffolds.

#### 4.1 Microgel inks

Microgel assemblies based on supramolecular interactions usually exhibit high viscosity, reversible shear thinning, creep resistance and rapid self-healing behaviors, which are suitable for extrusion-based 3D printing. Microgel assemblies based on interparticle hydrogen bonding or host-guest recognition may break up to flow under shearing/extruding, and then rapidly recover to the gel state once the shearing vanishes after extruding out of the nozzle. Meanwhile, the non-covalent interactions between microgels synergistically provide great resistance against creep, which is important for the fidelity and stability of printed structures.<sup>119</sup> Therefore, microgels can be applied as bioinks for 3D printing of constructs with multimodal and functional structure properties. For this purpose, balanced printability, high fidelity, and biocompatibility are highly desired.<sup>120</sup> Fu *et al.* prepared microgels with controllable size by repeatedly extruding and fracturing crosslinked CHMA/PVA hydrogels through nozzles<sup>12</sup> (Fig. 8a). The obtained microgels have irregular shapes and abundant hydroxyl groups that can establish numerous hydrogen bonds between hydrogel microparticles, which works with geometric jamming of the microparticles to form extrudable microgel hydrogels. The microparticle hydrogels undergo shear thinning and rapid self-healing into hydrogels after unloading. The microgel hydrogels have good mechanical stability and creep resistance, which provide outstanding printability and fidelity. The microgels have been used as inks to build a variety of bionic structures, which has excellent self-supporting, high aspect ratio and complex structures (Fig. 9b).<sup>121</sup>

Dynamic cross-linking reactions among microgels have been utilized to assemble microgels for extrusion bioprinting with great printability, microporosity, tissue-adhesion, and self-healing.<sup>122</sup> Feng *et al.* proposed a new strategy to prepare dynamic cross-linked microgel assembly (DC-MA) bioink (Fig. 10a). By using a droplet microfluidic device, methacrylate and phenylboronic group modified hyaluronic acid (HAMA-PBA) and methacrylic gelatin (GelMA) were crosslinked to produce microgels, and then the dynamic crosslinker (dopamine modified hyaluronic acid, HA-DA) was assembled into the DC-MA bioink to strengthen interactions between microgels through dynamic covalent bonds while maintaining the relatively low mechanical modulus of microgels in order to achieve high printability, shape-fidelity and cell viability.<sup>32</sup> The addition of dynamic



Fig. 9 (a) Self-healing pre-cross-linked hydrogel microparticle (pCH $\mu$ Ps) inks; (b) a variety of bionic structures. Reproduced with permission from ref. 12. Copyright 2020 John Wiley and Sons.

crosslinking agent (HA-DA) also improved the microporosity, tissue adhesion and self-healing of DC-MA bioink, which is beneficial for tissue engineering and regenerative medicine applications.

Microgels can act as sacrificial inks to improve cell infiltration and migration in scaffolds, while maintaining the printability of the microgel inks. Seymour *et al.* blended UV-crosslinkable gelation methacryloyl (GelMA) microgels with sacrificial gelatin microgels to obtain composite inks high void fraction by optimizing the ratio of GelMA to sacrificial gelatin microgels.<sup>27</sup> It was observed that human umbilical vein endothelial cells (HUVEC) seeded onto printed constructs migrated into the microgel inks depending on the void fraction. This strategy has potential for applications in 3D printing and tissue engineering.

Many 3D printing structures by using microgel (JM) bioinks may gradually lose mechanical properties in the long term, in comparison to natural soft tissues,<sup>36,124,125</sup> which limits their applications in tissue engineering. To address this problem, microgel particles with a high swelling ratio are dissolved in a second monomer solution to integrate the microgels together to produce microgel-based biphasic (MB) bioinks with both printability and fidelity. Amstad *et al.* synthesized poly(2-acrylamido-2-methyl-propanesulfonic acid) (PAMPS) microgels by inverse emulsion polymerization, and mixed them with a second monomer solution that is comprised of AAm monomers, initiators, and cross-linkers to create double network



Fig. 10 Microgel inks. (a) Dynamic cross-linked microgel assembly (DC-MA) bioink. Reproduced with permission from ref. 32. Copyright 2020 John Wiley and Sons. (b) Double network granular hydrogel (DNGH) inks. Reproduced with permission from ref. 123. Copyright 2022 American Chemical Society.

granular hydrogels (DNGHs) (Fig. 10b).<sup>123</sup> The obtained hydrogels can bear tensile loads up to 1.3 MPa. Zhao *et al.* prepared various microgels by ball milling, and polymerized the same monomers in the presence of microgels to generate particle-based double-network (P-DN) hydrogels.<sup>17</sup> The hydrogels show excellent adhesion and temperature sensitivity. This strategy can be used to print multi-functional hydrogel structures with high mechanical properties and strong adhesion to various materials.

Microgel-based biphasic (MB) bioinks can be combined with different types of cells to form a heterogeneous cell micro-environment in a single printed fiber.<sup>126</sup> Zhang *et al.* swelled sodium alginate microgels or GelMA microgels containing cells into GelMA solution to obtain tightly stacked biological ink<sup>127</sup> for printing 3D complex structures including nose, ear, bronchus and brain models with high shape fidelity. In MB bioink, the cell density was increased locally through a space cell pattern, which accelerated cell reorganization and vascularization, and further promoted the functional maturity of printed liver tissue constructs. In general, the MB bioink has mechanical adjustability, hyperelasticity and a heterogeneous microenvironment,<sup>128,129</sup> providing new possibilities for 3D bioprinting in biomedical applications such as tissue engineering and soft robots.

#### 4.2 Supporting bath

During conventional extrusion-based 3D printing, the ink is usually layer-by-layer deposited on the substrate and then further cross-linked to improve the shape fidelity and stability of the designed structure, and has therefore limited the selection of ink materials and the construction diversity of complex architectures such as human organs or tissues.<sup>130,131</sup> To overcome this shortcoming, bath-supported 3D printing has been applied to the construction of complex structures.<sup>132</sup> Different optimized bath materials have been developed to negate the effects of surface tension, gravity, and particle diffusion to support and fix the extruded ink, and firm the printed shapes.<sup>133,134</sup> Among these bath materials, the supramolecular assembled microgel bath has a high water content, transparency, and

self-healing, and prompts a smooth transition between fluid and solid states, which is an ideal medium for bath-supported 3D printing.<sup>135,136</sup> Many studies have shown that there are different yield stress support baths for the embedding bioprinting of hydrogels, including Carbomer, alginate particles, and gelatin microgel, *etc.*

Carbomer is a kind of supramolecular polyacrylic acid (PAA) polymer. The carboxylic groups on the molecular chain can firmly grasp water through hydrogen bonding. It shows a sol to gel transition in aqueous solution as the pH is raised above its  $pK_a$  (about 5.5).<sup>137</sup> Carbomer microgel has been widely used as a 3D printing supporting bath due to its stable, tunable viscoelasticity, and rheological behavior in a biological environment.<sup>138,139</sup> Serpooshan *et al.*<sup>140</sup> used Carbomer as the support bath and gelatin-methacryloyl (GelMA) as the 3D printing bioink to create a 3D hydrogel structure with high fidelity and biocompatibility through embedded bioprinting technology, further expanding the application of bioprinting soft tissue construction in various biomedical fields. Huang *et al.*<sup>141</sup> developed a Carbomer microgel supporting material as a bath to support the 3D structure constructed by gelatin-alginate ink, which avoids the instantaneous gelation of each printed layer and nozzle clogging caused by the resultant surface tension. It has been realized as the overall 'printing-then-gelation', which is suitable for building a variety of homogeneous soft structures. Angelini *et al.*<sup>142</sup> generated several complex structures by writing in a Carbomer microgel bath, including a 4 cm-long model of DNA, a thin-shell model and a complex vascular network. It's possible to write and grow living tissue cells in the microgel supporting bath and the jammed microgel provided stability and versatility in a simple framework that can be integrated into a powerful platform in the application of bioprinting soft tissue constructs in various biomedical fields.

The alginate chain is rich in mannuronic acid (M) and glucose uronic acid (G) units. In aqueous solution, the G blocks in different alginate chains can coordinate with multivalent cations (such as  $Ca^{2+}$ ,  $Co^{2+}$ ,  $Cu^{2+}$ ) to form non-covalent crosslinks between alginate chains, thus generating alginate hydrogels.<sup>143</sup>

As commonly used as a 3D printing supporting bath, alginate microgels show many advantages like cell friendliness, high transparency for realtime monitoring of printing, and can be removed by non-toxic, delicate procedures after printing. Alsberg *et al.*<sup>144</sup> presented a 3D printing strategy in which a bioink rich in stem cells was printed into a support bath comprised of alginate microgels prepared by double crosslinking, oxidation and ionic crosslinking of methacrylate alginate (OMA). The microgel support medium showed similar properties to Bingham plastic fluid, maintaining high-resolution printing of human bone marrow mesenchymal stem cells (hMSCs). Dvir *et al.*<sup>145</sup> used a mixed material comprised of calcium-alginate nanoparticles and xanthan gum as a supporting bath for the printing of extracellular matrix-based biomaterials, allowing high-resolution printing as low as 10 microns to manufacture complex structures and cell structures. It has been proved that the mixed medium can support at least 18 hours of long-time accurate printing. All these characteristics make it a promising supporting medium for 3D printing of tissues and organs. Ozbolat *et al.*<sup>146</sup> studied the feasibility of using human mesenchymal stem cell (hMSC) spheres with an alginate microgel support bath for aspiration-assisted freeform bioprinting (AAfB), which has achieved unprecedented positioning accuracy, and improved the fusion efficiency of bioprinting in alginate microgels with different particle sizes. These studies demonstrated the potential of using alginate microgels as a support bath, which can be used in many different applications, including free bioprinting of spheres, cell loaded hydrogels and unstructured inks, to form viable tissue structures.

Besides, gelatin is a partially hydrolyzed collagen with excellent biocompatibility and degradability, which is widely used in many 3D cell culture, tissue engineering and drug delivery applications. The gelation process of gelatin microgels

is thermally reversible.<sup>147</sup> Due to the weak interaction between chains, it can automatically transform into a hydrogel at low temperature and reversibly change into a liquid state when heated, which has been widely used in supporting bath materials. For example, Huang *et al.*<sup>148</sup> used the cross-linked composite hydrogel filled with gellan and gelatin microgels with a self-thinning property as the matrix bath to support the fabrication of 2D and 3D fluid network channels to increase the metabolic activity of living cells in the cross-linked matrix. The composite microgel matrix has sufficient mechanical strength to maintain the mechanical integrity of the structure during the removal of sacrificial materials. This method has potential for *in vitro* and *in vivo* applications, and may be particularly suitable for chip-based systems. Lee *et al.*<sup>138</sup> proposed a method of 3D biological printing collagen directly by precisely controlling the composition and microstructure (Fig. 11). They used the freeform reversible embedding of suspended hydrogels (FRESH) to design the composition of the human heart at various scales from capillaries to the whole organ in the thermo-reversible gelatin microgel supporting bath, which proved that FRESH v2.0 collagen printing can be used as a platform to build advanced tissue scaffolds for various organ systems.

## 5. Applications of supramolecular assemblies of microgels

Microgels have been used as basic units as vehicles to carry drug, factors, and cells, and serve as materials for the fabrication of scaffolds and constructs with biomimetic structures and functionalities. The manufacturing and assembly process of supramolecular microgels is generally fast, biocompatible and non-toxic.<sup>149</sup> Due to the dynamic and reversible interactions,



Fig. 11 A thermo-reversible gelatin microgel as the supporting bath for FRESH printing. Reproduced with permission from ref. 138. Copyright 2019 The Authors.

supramolecular microgels always show excellent self-healing, injectability, flexibility and biocompatibility, which are crucial for biological and medical applications.<sup>40,149</sup> Recent progress in supramolecular microgels for biomedical applications such as cell culture, drug delivery, antibacterial and tissue engineering is summarized in the following sections.

### 5.1 Cell culture

Various strategies have been proposed to culture cells in a 3D environment simulating the microenvironment *in vivo*, named 3D cell culture, among which the scaffold-based approach has been extensively studied and developed.<sup>150</sup> Supramolecular microgel assemblies have been used as scaffolds for 3D cell culture by encapsulating cells inside or inoculating cells on the surface. Microgel assemblies usually have a modulus similar to human tissue. The mechanical and chemical properties can be adjusted as needed to accurately simulate the natural 3D cell microenvironment determined by the ECM with a high water content so as to protect the encapsulated cells from shear force during injection or printing.<sup>151,152</sup> In addition, compared with bulk hydrogels, microgels have high porosity and high surface area to mass ratio due to their microscale size, which not only provides enough growth space for cells, but also facilitates rapid nutrient/waste exchange and maintains high cell vitality.<sup>19</sup>

There are many supramolecular biopolymers used to prepare microgels for 3D cell culture. For example, chitosan-based microgels have been applied as microcarriers for cell culture. The water soluble, UV crosslinkable and injectable *N*-methacryloyl chitosan (N-MAC) was synthesized through a one-step chemically selective *N*-acylation reaction, which allows for rapid, robust and cost-effective production of patterned cell loaded polysaccharide microgels with unique amino groups, as a building block for cell culture and local and continuous protein delivery.<sup>153</sup> PEG-based biocomposite microgels have been widely used in the field of biological applications. The host-guest supramolecular interaction is introduced into the PEG microgel to provide a reversible non-covalent bond and generate a permeable interpenetrating network to form a polyethylene glycol maleimide (PEG-MAL) microgel scaffold.<sup>75</sup> The porous structures of the scaffold can enable rapid migration of THP-1 monocytes, which can be used to simulate a natural ECM environment to study the immune cell interaction in the matrix.

Different technologies have been developed to rapidly assemble a heterogeneous 3D cell microenvironment with microgels, including droplet microfluidics, bioprinting, microforming and stop-flow lithography.<sup>154</sup> Among them, droplet microfluidics has many advantages, such as accurate diameter control, rapid preparation speed and controllable microsphere structure, which makes the delivery of cells and drugs more flexible, efficient and controllable. It has proved most suitable for continuous high-throughput production of monodisperse spherical microgels.<sup>155</sup> For example, Li *et al.* combined the microdroplet-array-based method with surface-wettability-guided assembly (SWGA) to guide the rapid assembly of heterogeneous 3D cell microenvironment arrays (Fig. 12a).<sup>156</sup> This method can accurately control the

shape, size, chemical concentration, cell density and 3D spatial distribution of multiple components, which provides a cost-effective solution to meet the growing needs of stem cell research. Besides, the method based on microfluidics was used to encapsulate single cells in the alginate layer of about 6 microns,<sup>157</sup> which has increased the proportion of microgels containing cells by 10 times, the encapsulation efficiency exceeding 90%, and helps keep the cells alive *in vitro* for three days. The intravenous injection of single encapsulated bone marrow stromal cells into mice could maintain the soluble factor provided by the donor *in vivo*. Single cells encapsulated in tunable microgels can be used in various tissue engineering and regenerative medicine applications (Fig. 12b).

### 5.2 Drug delivery

Compared with chemically crosslinked hydrogels, dynamically crosslinked supramolecular microgels have excellent biocompatibility, biodegradability and a long gelling period. The shear-thinning and self-healing properties of the supramolecular microgel assembly make it injectable and implantable,<sup>40</sup> and it can be used as a carrier for local drug delivery in a minimally invasive manner. Moreover, because the microgels have controllable high porosity, when being used to deliver drugs, the drug release rate *in vivo* can be adjusted by controlling the porosity of microspheres.<sup>155</sup> It provides unique advantages for the polymer-based drug delivery system: adjustable size from nanometer to micrometer, large surface area of multivalent biological coupling, and internal network of biological molecule binding.<sup>158</sup>

A wide range of small molecules, proteins and nucleic acid drugs have been encapsulated and released in a controlled manner using supramolecular microgels. Anionic copolymer microgels based on *N*-isopropylacrylamide and acrylic acid can load a cationic local anesthetic, bupivacaine. The microgel was compounded with an *in situ*-gelling hydrogel network cross-linked by hydrazide-aldehyde supramolecular chemistry to form hydrogel-microgel soft nanocomposites.<sup>159</sup> These nanocomposite hydrogels can provide sustained drug release for up to 60 days, which is significantly longer than the time (<1 week) that can be achieved by using hydrogels or microgels alone. In addition, microgels fabricated *via* microfluidics are used to encapsulate interleukin-10 (IL-10).<sup>8</sup> The degradation and release rate of the microgels can be controlled by the crosslinker. The microgels are injected into a rat model of myocardial infarction (MI), where the released IL-10 reduces macrophage density in 1 week, and improves scar therapy, ejection fraction, cardiac output, and the size of vascular structures in 4 weeks.

The soft nanocomposite hydrogels with long-term local drug delivery have great potential for clinical use. Host-guest supramolecular microgels based on CD have become a promising nanomaterial in biomedical drug delivery applications, benefiting from the complexing ability of CD with a wide range of drugs and hydrophobic molecules.<sup>160</sup> Qian *et al.*<sup>161</sup> combined the hydrophobic drug paclitaxel (TAX) and macrocyclic molecule  $\beta$ -CD with the poly-acrylic acid hydrogel skeleton, and then



**Fig. 12** Cell culture. (a) The microdroplet-array-based method with SWGA to guide the assembly of heterogeneous 3D cell microenvironment arrays. Scale bar, 50  $\mu\text{m}$ . Reproduced with permission from ref. 156. Copyright 2016 John Wiley and Sons. (b) A method based on microfluidics used to encapsulate single cells. Reproduced with permission from ref. 157. Copyright 2017 Springer Nature.

cross-linked it into PAA- $\beta$ -CD/PAA-TAX nanogels with multiple host-guest contents, which can be used as a new delivery carrier of mucosal adhesive to extend the residence time of TAX in the cervix and reverse the MDR of tumors to improve drug efficiency, and enhance the therapeutic effect of cervical cancer. Si *et al.*<sup>162</sup> designed a supramolecular nanogel for RNase cytoplasmic delivery, and the nanogel was prepared by host-guest interaction between azobenzene (Azo) and  $\beta$ -cyclodextrin ( $\beta$ -CD) conjugated with poly(L-glutamic acid)-*graft*-poly(ethylene glycol) methyl ether (PLG-*g*-mPEG). RNase can be loaded into nanogels under mild aqueous conditions. Due to the conformational transformation of azo triggered by UV light, the cross-linking points based on Azo/ $\beta$ -CD recognition were destroyed, which thus ensured the hypoxia sensitive release of nanogels to goods in tumors with NTR overexpression. The hypoxia sensitive supramolecular nanogel provides a universal platform for the delivery of RNase, highlighting its applicability in cancer treatment (Fig. 13a).

Stimulation responsiveness is another important feature of supramolecular microgel assemblies, which can respond to single or multiple exogenous/endogenous physical or biochemical stimuli (such as: heat, light, magnetic/electric field, mechanical force, pH value, redox potential, *etc.*).<sup>40</sup> Through fine adjustment of the gel-sol phase transition or volume expansion/contraction of microgels, it can be used as intelligent carriers for on-demand drug delivery. According to specific body parts or pathological conditions (such as inflammation), the loaded therapeutic goods can be accurately released in a continuous manner to improve the therapeutic effect. Song and colleagues<sup>163</sup> developed a bionic microgel with tumor microenvironment pH response characteristics to achieve co-delivery and controlled release of paclitaxel (PTX) and IL-2 (Fig. 13b). The 2-hydroxypropyl- $\beta$ -cyclodextrin (HP- $\beta$ -CD) is compounded with two chitosan derivatives with opposite charges to prepare supramolecular nanocomposite microgels, which are used to embed the anticancer drug paclitaxel, and can precisely control

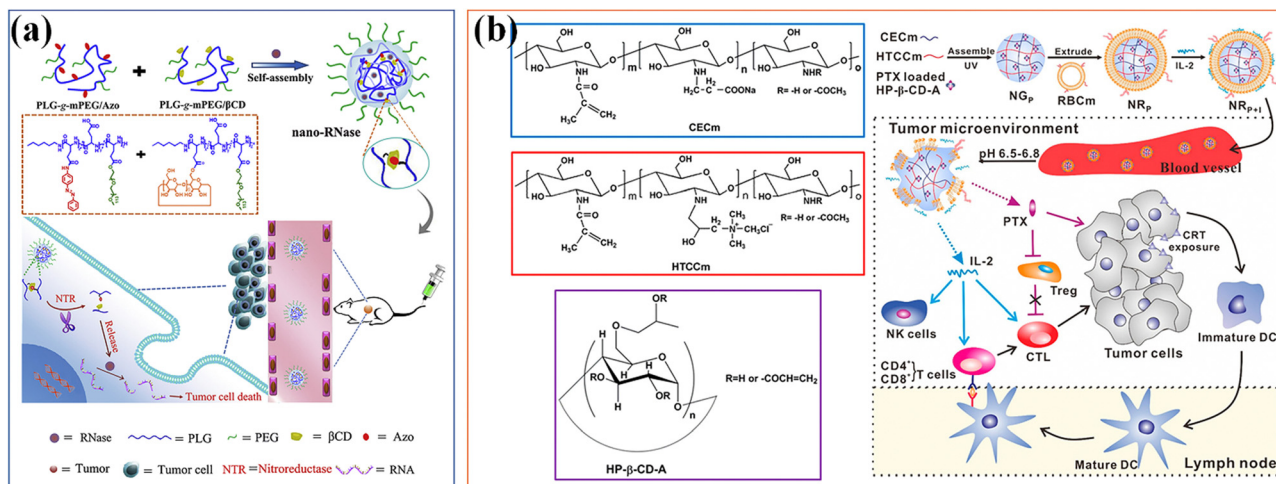


**Fig. 13** Drug Delivery. (a) A supramolecular nanogel for RNase cytoplasmic delivery. Reproduced with permission from ref. 162. Copyright 2020 Elsevier. (b) A bionic microgel with tumor microenvironment pH response characteristics to achieve controlled release and delivery of paclitaxel (PTX) and IL-2. Reproduced with permission from ref. 163. Copyright 2017 American Chemical Society.

the pH response ability to the weak acidic tumor microenvironment. The RBCm is further coated on the nanogels to enhance the adsorption, protection and delivery of physically and chemically unstable IL-2. The drug released in response can effectively play its role and achieve a promising synergistic anti-tumor effect. Another batch of supramolecular hydrogels used as drug delivery platforms are based on thermal gel polymers with thermal responsiveness.<sup>44</sup> Antoniuk *et al.*<sup>164</sup> used electrostatics and host-guest self-assembly to coat positively charged  $\beta$ -cyclodextrin polymers in PNIPAAm microgels to prepare host-guest supramolecular hydrogels through inclusion complexation with adamantane substituted dextran to generate a  $\beta$ -cyclodextrin adamantane ( $\beta$ -CD-Ada) inclusion complex. Due to the synergistic effect between the shrinkage of microgels and the dissociation of  $\beta$ -CD-Ada crosslinks at higher temperatures, the hydrogels exhibit a completely reversible thermally driven gel-sol transition at the temperature range from 37 to 41 °C, opening up attractive prospects for their potential applications in biomedical applications such as stimulation responsive drug delivery.

### 5.3 Antibacterial

Bacterial infection may lead to serious diseases, including pneumonia, tuberculosis, septicemia, cholera and meningitis, which threaten global human health and are the main causes of death worldwide. Bacterial infection is mainly caused by bacterial biofilm formed by initial bacterial attachment and subsequent bacterial cell proliferation and colonization. In recent years, due to the enhancement of antibiotic resistance, it is urgent to combine antibiotics with other polymers to improve their antibacterial properties or develop new antibacterial drugs to deal with infections in biomedical environments.<sup>45,165</sup> Supramolecular microgels can be used as delivery carriers of antibiotics, or directly combined with drugs to form new antibacterial drugs or coatings for application in biological antibacterial products, and have been recognized as a promising method to solve multi drug resistant bacteria.

Other than drugs, commonly used antimicrobial agents include quaternary ammonium compounds (QACs),<sup>166,167</sup> antimicrobial peptides (AMPs),<sup>168–170</sup> and antimicrobial enzymes (AMEs).<sup>171,172</sup> Many studies have involved the delivery of antimicrobial agents using supramolecular microgel systems.<sup>45,173</sup> Self-assembled polyethylene glycol (PEG) and polyethylene glycol-*co*-acrylic acid (PEG-AA) microgels can regulate surface cell adhesion on a micron scale comparable to the size of bacteria, and are used for local storage/release of antimicrobial agents to inhibit bacterial colonization on synthetic surfaces.<sup>174</sup> Due to electrostatic interactions, the microgels can load cationic antimicrobial peptides (L5). The load in PEG-AA microgels was significantly higher than that in pure PEG microgels. These microgels can be deposited through a nonlinear visual self-assembly process, hinder bacterial colonization, and reduce infection rates associated with biomaterials.

Hydrophilic microgels and nanogels can be utilized to encapsulate and deliver hydrophobic antibacterial agent<sup>175</sup> that is urgently needed to tackle antibiotic resistance through nano-injection. Nanogels based on poly(*N*-isopropylacrylamide-*co*-*N*-[3-(dimethylamino) propyl] methacrylamide) and poly(NIPAM-*co*-DMAPMA), for example, are quaternized with 1-bromododecane to form hydrophobic domains inside the network through self-assembly of aliphatic chains (C12). Triclosan is loaded within the hydrophobic domains serving as containers to load Triclosan inside the nanogels, and the nanogels can adhere to the bacterial cell wall *via* electrostatic interactions and induce membrane destruction *via* the insertion of the aliphatic chains into the cell membrane. Thus, Triclosan can be injected into the cell through the destroyed membrane to dramatically increase the effective Triclosan concentration at the bacterial site. As a result, both the minimal inhibitory concentration and minimal bactericidal concentration against the Gram-positive bacteria *S. aureus* and *S. epidermidis* are reduced by 3 orders of magnitude, in comparison with free Triclosan. The strategy achieves synergetic physical destruction

and active nano-injection, which significantly enhances the antimicrobial efficacy. The designed nanoinjection delivery system shows great promise for combating antimicrobial resistance, and extending applications of hydrophobic drugs delivery for previously challenging applications.

Nanogels with an inherent antibacterial part have been studied.<sup>45</sup> The positively charged part causes physical damage to the bacterial cell membrane, which is one of the main antibacterial mechanisms of functional nanogels. The strong charge interaction leads to pore formation and changes in membrane permeability, eventually leading to bacterial cell death.<sup>176</sup> Among different cationic compounds for applications to functionalize nanogels, quaternary ammonium salt (QAS) is the most explored. QAS-based PNIPAM (QAS-PNIPAM) microgels<sup>177</sup> are synthesized and utilized to modify the surface of a range of materials including metal, plastic, and elastomer. Bacterial culture on QAS-PNIPAM microgel-modified surfaces shows a bactericidal efficiency of nearly 100% (Fig. 14a). The highly efficient bactericidal performance of the QAS-PNIPAM microgel film is attributed to the cationic QAS component. Moreover, the microgel film is robust and cyto-compatible. The cytocompatibility of QAS-PNIPAM microgel thin films can be further improved by modifying with a glycopolymer containing sulfonate groups *via* attractive electrostatic interactions (Fig. 14b).<sup>178</sup> Introduction of the sugar units improves the cytocompatibility of the microgel film without compromising its bactericidal efficacy.

In addition, AMPs interact with bacteria through non-specific (electrostatic) mechanisms, and have potent antibacterial,

anti-inflammatory and other host defense properties.<sup>173</sup> A series of polypeptide nanogels (PNGs) have been prepared by using coordination assisted self-assembly of mannose-conjugated AMPs, with poly(arginine)-mannose as the ligand, and  $Zn^{2+}$  ions as a metal ion source, which can minimize the toxicity of the original polypeptide without compromising antimicrobial activity.<sup>179</sup> PNG shows potential bactericidal effects on *Staphylococcus aureus* and *Escherichia coli*. Compared with the original polypeptide, PNG exhibits higher cell viability (higher than 80%) on mammalian cells (Fig. 14c).

#### 5.4 Tissue engineering

Biotissues and organs are complex systems composed of ECMs, different cells, proteins, and signaling molecules with highly ordered structures. Biofabrication strategies have been developed to engineer 3D tissue models *in vitro* by mimicking the structure and function of native tissues. The key is to precisely deposit and assemble materials and cells with biomimetic spatiotemporal control.<sup>180</sup> Precise control over biophysical and biochemical cues is required to direct cell growth and tissue regeneration.<sup>181</sup> Regenerative medicine demands controlled delivery of growth factors and other active substances to promote cell adhesion and guide cell differentiation and tissue formation. Nanogels and microgels could be added to tissue scaffolds for local encapsulation and delivery of bioactive species, modifying their inner architecture, texture and mechanical properties, for regulating cell behavior, and tissue regeneration applications.<sup>37</sup> Specifically, nanogels can be fabricated into architectures for regenerating nerve, vessels, cardiac

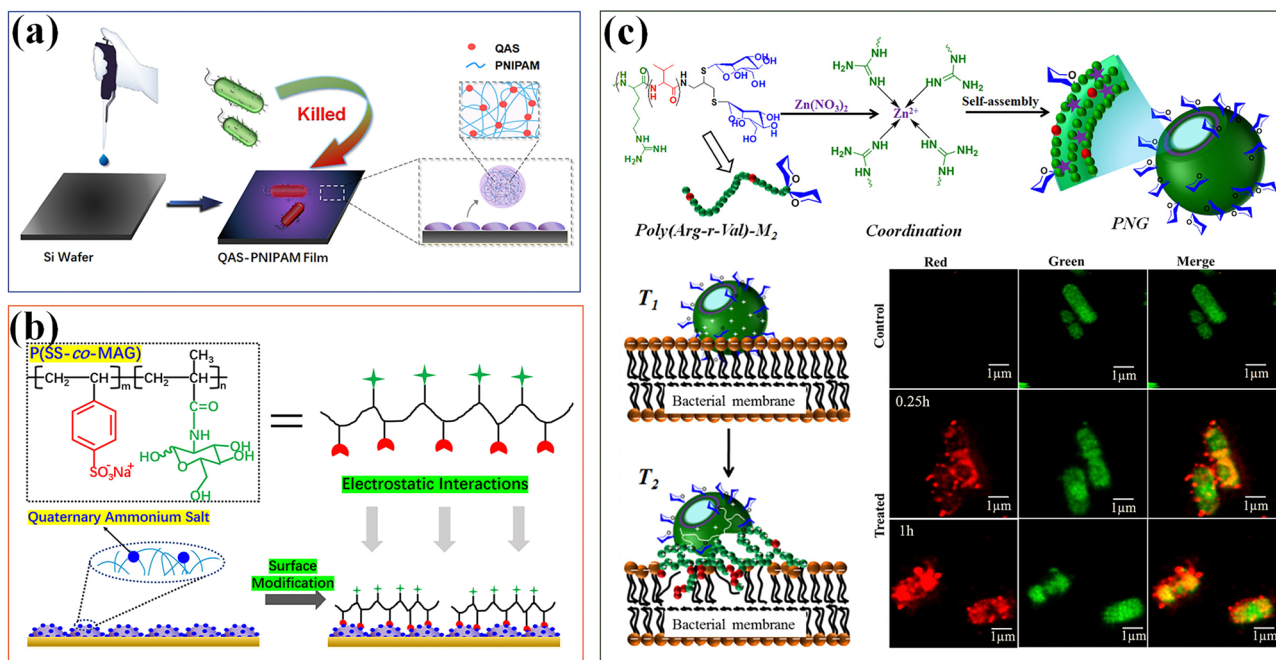


Fig. 14 Antibacterial. (a) The antibacterial thin films modified by QAS-based PNIPAM (QAS-PNIPAM) microgels. Reproduced with permission from ref. 177. Copyright 2020 American Chemical Society. (b) Modification of quaternized QPM films with P(SS-co-Mag) *via* electrostatic interactions has improved the cytocompatibility. Reproduced with permission from ref. 178. Copyright 2020 Elsevier. (c) Polypeptide nanogels (PNGs) with mannose-conjugated AMPs show potential bactericidal effects. Reproduced with permission from ref. 179. Copyright 2019 American Chemical Society.

tissue, liver, urothelium and urethral muscle tissues. Multidisciplinary approaches to design nanogels have been employed to meet the diverse needs of regenerative medicine, including active ingredient formulation, controlled release, nanomechanics, tissue engineering and scaffolding with the common purpose of developing clinically relevant tools for the regeneration of complex tissues.

Tissue engineering scaffolds play an important role in filling tissue defects, providing mechanical support, promoting cell infiltration, growth and metabolism, achieving the required interactions between cells, releasing encapsulation factors (such as growth factors, chemokines and cytokines) and other functions, so that cells can adhere to biological material scaffolds to form cell-material composites. The compound is implanted into the damaged parts of tissues or organs of the body.<sup>182</sup> With gradual degradation and absorption of biomaterials in the body, the implanted cells continue to proliferate and secrete extracellular matrix *in vivo*, eventually forming the corresponding tissues or organs to achieve the purpose of repairing trauma and rebuilding functions.<sup>183</sup> In the past three decades, hydrogel materials have been widely applied in tissue engineering scaffolds for tissue repair and regeneration due to their high-water content, excellent biocompatibility, and biological modulus close to that of tissues and organs, which can be engineered to simulate the natural tissue environment.

Supramolecular microgels are promising for repair and regeneration of different types of tissues and organs due to

their highly hydrated nature, tunable microporous structure, ability to encapsulate bioactive factors, and tailorable properties such as stiffness and composition.<sup>34</sup> In particular, reversible supramolecular interactions between microgels make the hydrogels injectable and self-healable.<sup>184</sup> Supramolecular microgels, as well as their composites with drug, factors, and cells, are ideal candidates for 3D printing ink to fabricate tissue engineering scaffolds with tunable properties to match those of target tissues.<sup>36</sup> Microgel-based tissue engineering materials have been recognized for regenerative medicine in the fields of cartilage, cardiac vascular tissue repair, neuron tissue engineering, *etc.*

Reconstruction of the cartilage defect structure through self-assembly of microgels has a promising application in cartilage tissue engineering and regenerative medicine.<sup>185</sup> Microgel assemblies provide a mechanical microenvironment to regulate stem cell chondrogenesis.<sup>186</sup> Gelatin/hyaluronic acid hybrid microgels with low, medium and high crosslinking densities are fabricated in microfluidic devices by Michael addition reaction between thiolated gelatin (Gel-SH) and ethylsulfated hyaluronic acid (HA-VS) with different substitution degrees of vinyl sulfone groups. The mouse bone marrow mesenchymal stem cells (BMSC) show a clear trend of differentiating into hyaline cartilage in microgels with a low crosslink density, and fibrocartilage in microgels with medium and high crosslinking densities. Besides, dynamic nanocomposite microgel assemblies are composited with cyclodextrin nanoparticles loaded



**Fig. 15** Tissue engineering. (a) BMSC-laden microgel assembly can repair cartilage *in vivo*. Reproduced with permission from ref. 187. Copyright 2021 John Wiley and Sons. (b) A two-component HA microgel assembly applied in cardiovascular tissue repair. Scale bar = 500  $\mu\text{m}$ . Reproduced with permission from ref. 20. Copyright 2018 John Wiley and Sons.

with kartogenin (KGN) and encapsulate BMSCs *via* droplet-based microfluidics and photo-crosslinking. The composite hydrogels are bottom-up assembled *via* dynamic crosslinking between dopamine-modified hyaluronic acid and phenylboronic acid groups on the microgel surface.<sup>187</sup> The microgel assemblies can avoid cell endocytosis, ensure high BMSC viability during cell culture, cryopreservation and injection process, and promote chondrogenic differentiation of BMSCs. Injection of the composite hydrogels into articular cartilage defects in animals leads to regeneration of articular cartilage (Fig. 15a). Moreover, injectable hBMSC-laden microgels can be assembled as building blocks into highly ordered tissue-like structures for long-term

maintenance and chondrogenesis.<sup>188</sup> Cell-laden microgels can be linked by using a 4-arm poly(ethylene glycol)-*N*-hydroxy-succinimide (NHS) crosslinker into a 3D construct, with the viability and cellular functions of encapsulated hBMSCs well preserved. This assembled microgel construct facilitates upregulation of chondrogenic markers in both gene and glycosaminoglycan (GAG) expression levels, and regeneration of hyaline-like cartilage and high content of type II collagen.

Cardiac vascular tissue repair aims at cardiac regeneration and vascular repair after injury or myocardial infarction. As a cardiovascular scaffold, microgels can effectively retain and/or deliver cells to affected tissues.<sup>189</sup> Mealy *et al.*<sup>20</sup> developed a



Fig. 16 Tissue engineering. (a) An adaptive microporous hydrogel (AMH) has been developed to treat nerve injury and nerve regeneration. Reproduced with permission from ref. 192. Copyright 2019 John Wiley and Sons. (b) The cell-laden OMA microgels are applied in the construction of artificial tissues and organs. Scale bar, 1 cm. Reproduced with permission from ref. 194. Copyright 2019 John Wiley and Sons.

two-component HA microgel assembly containing protease-cleavable and stable microgels through host-guest interaction, showing shear thinning and self-healing properties, making it easy to inject. More importantly, after injection into the myocardial wall of male Wistar rats with myocardial infarction, the lysable microgels showed significantly accelerated degradation due to the high protease activity under myocardial infarction conditions, while the stable microgels still existed in an undegraded spherical form. The composite properties and high porosity of the two-component granular hydrogel provide unique disease-dependent behavior and high-level cell invasion after injection into myocardial tissue (Fig. 15b). In addition, heparin-modified Pluronic F127 supramolecular nanogels containing basic fibroblast growth factor and VEGF165pDNA introduce proteins and genes into EPCs to promote neovascularization in animal models of limb ischemia,<sup>190</sup> effectively promoting the vascularization of female BALB/c mice with femoral artery resection, and form artificial blood vessels.

Nerve degeneration, scar formation and loss of communication between neurons and cells are the main problems of nerve injury. Various neural tissue engineering methods based on supramolecular microgels have been developed to treat nerve injury.<sup>191</sup> Hsu *et al.*<sup>192</sup> propose an adaptive microporous hydrogel (AMH), in which high, medium and low concentrations of neuronal growth factor are loaded into negatively charged GelMA microgels, and then mixed with an equal volume of positively charged chitosan methacrylate microgels. The interconnected injectable porous scaffold constructed by electrostatic interaction has suitable micropores to promote cell migration, provides mechanical support, and transports biomolecular clues to manage cell adhesion and growth. Chitosan degradation products have been shown to contribute to peripheral nerve regeneration, inducing a significant bridging effect (axon growth of 4.7 mm) on peripheral nerve defects in SD rats (Fig. 16a). Zhao *et al.*<sup>193</sup> developed a bifunctional microgel to simultaneously reduce the concentration of  $\text{Ca}^{2+}$  and glutamate in the extracellular environment and inhibit excessive  $\text{Ca}^{2+}$  influx. The microgels are formed by hydrogen bonding between dextran and loaded  $\Omega$ -conotoxin GVIA (DexGVIA). The DexGVIA significantly accelerates the recovery of motor function in spinal cord injury rats by reducing the injury cavity, protecting neurons and glial cells from injury, improving the continuity and integrity of the spinal cord, and promoting nerve tissue regeneration.

Human organs are composed of complex tissues and have gradient characteristics on various length scales, which is the basis of morphology and function. Microgels have been widely used as building blocks of 3D printed artificial tissues and organs due to their adjustable physical properties, cell adhesion and printability.<sup>195,196</sup> So far, many studies have proved the application of cell-laden microgels in the construction of artificial tissues and organs.<sup>197</sup> Dual-crosslinkable alginate microgels comprised of oxidized and methacrylated alginate (OMA) are synthesized to encapsulate cells. The cell-laden OMA microgels are directly assembled into well-defined 3D shapes and structures under low-level ultraviolet light. The stem cell-laden OMA microgels can be successfully cryopreserved for

long-term storage and on-demand applications (Fig. 16b). The recovered encapsulated cells maintained equivalent viability and functionality to the freshly processed stem cells. The cell-laden microgels can be assembled into complicated 3D tissue structures *via* freeform reversible embedding of suspended hydrogel (FRESH) 3D bioprinting.<sup>194</sup> Then, the second generation of FRESH v2.0 3D bioprinting technology was developed to design the tissue composition of the human heart on multiple length scales.<sup>138</sup> Through the use of collagen<sup>198</sup> a tri-leaflet heart valve 28 mm in diameter and a human heart chamber of newborn scale were printed,<sup>199</sup> and it has proved that FRESH v2.0 collagen printing can be used as a platform to build advanced tissue scaffolds for various organ systems. This bottom-up strategy provides a powerful and highly scalable tool for fabrication of customized and biomimetic 3D tissue constructs.<sup>200</sup>

## 6. Conclusions and perspective

In summary, supramolecular microgel assemblies based on non-covalent physical interactions, including host-guest interactions, hydrogen bonding, metal coordination and electrostatic interaction, *etc.*, have great potential for biomedical applications. The alternative integration of bioactive microgels with other functional substances can be applied to drug delivery and release, regenerative medicine, and antibacterial applications, *etc.* Due to their dynamic self-thinning and self-healing, supramolecular microgels show injection and designability, and can be used as 3D printing bioinks or a supporting bath to fabricate tissue engineering scaffolds and artificial organs. The micron size and macro porosity of microgels are beneficial for cell migration and drug diffusion, which is conducive to cell culture, drug delivery and tissue regeneration, which show huge prospects in the biomedical field.

Despite many excellent properties of supramolecular microgel assemblies, there are still many challenges and unmet demands that remain to be addressed. First, massive production of multifunctional microgels is desired to fabricate macro 3D structures by using microgels as building blocks. However, most current manufacturing methods are difficult to simultaneously achieve both high yield and size uniformity of microgels. It is necessary to develop new methods or improve existing technologies to realize high-throughput production, long-term storage and transportation of cell-encapsulated microgels. Second, the degradation rate is preferred to match the regeneration rhythm of tissue regeneration. Besides, the cytotoxicity of degradation by-products may raise problems for applications of supramolecular microgels in cell culture and drug delivery, including possible host immune reactions. It is very important to explore non-toxic, controllable degradation functional microgels for targeted drug delivery through drug matrix affinity supramolecular design.

In addition, supramolecular microgels composed of natural biomaterials are usually cross-linked by non-covalent interactions, and have weak mechanical properties that usually

affect the structural integrity of engineering structures. Synthetic biomaterials can provide higher mechanical strength and structural integrity, and become an appropriate choice for load-bearing tissues and nerve conduits. It is necessary to build hybrid microgel tissue engineering scaffolds by combining the advantages of natural and synthetic entities in a single construct. A second network can be incorporated during post-processing to form an interpenetrating network to further stabilize the structures. Moreover, the directional assembly of microgels into arbitrary 3D structures is still in its infancy. Using biomaterials with biocompatibility, heterogeneity and versatility to integrate various biophysical/biochemical clues into the microgels or use signal factors secreted by encapsulated cells or peripheral tissue cells may help promote the spatiotemporal assembly of microgels *in vivo*. In general, great opportunities and challenges need extensive studies and exploration to broaden the biological applications of supramolecular microgel assemblies for forefront research and clinical applications.

## Conflicts of interest

There are no conflicts to declare.

## Acknowledgements

This study was supported by the National Natural Science Foundation of China (51873224), and the Ministry of Industry and Information Technology of China (TC190H3ZV/1).

## References

- J. P. Newsom, K. A. Payne and M. D. Krebs, *Acta Biomater.*, 2019, **88**, 32–41.
- X. Tong and F. Yang, *Adv. Healthcare Mater.*, 2018, **7**, 1701065.
- A. Khademhosseini and R. Langer, *Nat. Protoc.*, 2016, **11**, 1775–1781.
- X. Tong and F. Yang, *Adv. Healthcare Mater.*, 2018, **7**, 1701065.
- Y. Kittel, A. J. C. Kuehne and L. De Laporte, *Adv. Healthcare Mater.*, 2022, **11**, 2101989.
- D. Xia, P. Wang, X. Ji, N. M. Khashab, J. L. Sessler and F. Huang, *Chem. Rev.*, 2020, **120**, 6070–6123.
- C. L. Hedegaard and A. Mata, *Biofabrication*, 2020, **12**, 032002.
- M. H. Chen, J. J. Chung, J. E. Mealy, S. Zaman, E. C. Li, M. F. Arisi, P. Atluri and J. A. Burdick, *Macromol. Biosci.*, 2019, **19**, 1800248.
- A. C. Daly, L. Riley, T. Segura and J. A. Burdick, *Nat. Rev. Mater.*, 2020, **5**, 20–43.
- T. Farjami and A. Madadlou, *Food Hydrocolloids*, 2017, **62**, 262–272.
- A. Sinclair, M. B. O'Kelly, T. Bai, H. C. Hung, P. Jain and S. Jiang, *Adv. Mater.*, 2018, **30**, 1803087.
- H. Zhang, Y. Cong, A. R. Osi, Y. Zhou, F. Huang, R. P. Zaccaria, J. Chen, R. Wang and J. Fu, *Adv. Funct. Mater.*, 2020, **30**, 1910573.
- T. J. Hinton, Q. Jallerat, R. N. Palchesko, J. H. Park, M. S. Grodzicki, M. H. R. H.-J. Shue, A. R. Hudson and A. W. Feinberg, *Sci. Adv.*, 2015, **1**, 1–10.
- F. A. Plamper and W. Richtering, *Acc. Chem. Res.*, 2017, **50**, 131–140.
- J. Xue, Z. Zhang, J. Nie and B. Du, *Macromolecules*, 2017, **50**, 5285–5292.
- A. S. Caldwell, G. T. Campbell, K. M. T. Shekiri and K. S. Anseth, *Adv. Healthcare Mater.*, 2017, **6**, 1700254.
- D. Zhao, Y. Liu, B. Liu, Z. Chen, G. Nian, S. Qu and W. Yang, *ACS Appl. Mater. Interfaces*, 2021, **13**, 13714–13723.
- Y. Xu, R. P. B. Jacquat, Y. Shen, D. Vigolo, D. Morse, S. Zhang and T. P. J. Knowles, *Small*, 2020, **16**, 2000432.
- J. M. de Rutte, J. Koh and D. Di Carlo, *Adv. Funct. Mater.*, 2019, **29**, 1900071.
- J. E. Mealy, J. J. Chung, H. H. Jeong, D. Issadore, D. Lee, P. Atluri and J. A. Burdick, *Adv. Mater.*, 2018, **30**, 1705912.
- L. R. Nih, E. Sideris, S. T. Carmichael and T. Segura, *Adv. Mater.*, 2017, **29**, 1606471.
- S. Jung and H. Yi, *Langmuir*, 2012, **28**, 17061–17070.
- J.-Y. Leong, W.-H. Lam, K.-W. Ho, W.-P. Voo, M.-F. X. Lee, H.-P. Lim, S.-L. Lim, B.-T. Tey, D. Poncelet and E. S. Chan, *Particology*, 2016, **24**, 44–60.
- J. E. Meiring, M. J. Schmid, S. M. Grayson, B. M. Rathsack, D. M. Johnson, R. Kirby, R. Kannappan, K. Manthiram, B. Hsia, Z. L. Hogan, A. D. Ellington, M. V. Pishko and C. G. Willson, *Chem. Mater.*, 2004, **16**, 5574–5580.
- K. Song, D. Zhang, J. Yin and Y. Huang, *Addit. Manuf.*, 2021, **41**, 101963.
- Y. Zhang, S. T. Ellison, S. Duravel, C. D. Morley, C. R. Taylor and T. E. Angelini, *Bioprinting*, 2021, **21**, 00121.
- A. J. Seymour, S. Shin and S. C. Heilshorn, *Adv. Healthcare Mater.*, 2021, **10**, 2100644.
- D. R. Griffin, W. M. Weaver, P. O. Scumpia, D. Di Carlo and T. Segura, *Nat. Mater.*, 2015, **14**, 737–744.
- H. Li, X. Li, P. Jain, H. Peng, K. Rahimi, S. Singh and A. Pich, *Biomacromolecules*, 2020, **21**, 4933–4944.
- K. Song, B. Ren, Y. Zhai, W. Chai and Y. Huang, *Biofabrication*, 2021, **14**, 015014.
- Z. Yu, J. Liu, C. S. Y. Tan, O. A. Scherman and C. Abell, *Angew. Chem., Int. Ed.*, 2018, **57**, 3079–3083.
- F. L. C. Morgan, L. Moroni and M. B. Baker, *Adv. Healthcare Mater.*, 2020, **9**, 1901798.
- H. Qi, M. Ghodousi, Y. Du, C. Grun, H. Bae, P. Yin and A. Khademhosseini, *Nat. Commun.*, 2013, **4**, 2275.
- K. Wang, Z. Wang, H. Hu and C. Gao, *Supramol. Mater.*, 2022, **1**, 100006.
- J. Xu, Q. Feng, S. Lin, W. Yuan, R. Li, J. Li, K. Wei, X. Chen, K. Zhang, Y. Yang, T. Wu, B. Wang, M. Zhu, R. Guo, G. Li and L. Bian, *Biomaterials*, 2019, **210**, 51–61.
- Q. Feng, D. Li, Q. Li, X. Cao and H. Dong, *Bioact. Mater.*, 2022, **9**, 105–119.

- 37 M. A. Grimaudo, A. Concheiro and C. Alvarez-Lorenzo, *J. Controlled Release*, 2019, **313**, 148–160.
- 38 M.-C. Tatry, P. Galanopoulou, L. Waldmann, V. Lapeyre, P. Garrigue, V. Schmitt and V. Ravaine, *J. Colloid Interface Sci.*, 2021, **589**, 96–109.
- 39 K. Marcisz, E. Zabost and M. Karbarz, *Appl. Mater. Today*, 2022, **29**, 101656.
- 40 S. Wang, P. J. Ong, S. Liu, W. Thitsartarn, M. J. B. H. Tan, A. Suwardi, Q. Zhu and X. J. Loh, *Chem. – Asian J.*, 2022, **17**, 202200608.
- 41 N. Mitrousis, A. Fokina and M. S. Shoichet, *Nat. Rev. Mater.*, 2018, **3**, 441–456.
- 42 M. Dirksen, C. Dargel, L. Meier, T. Brändel and T. Hellweg, *Colloid Polym. Sci.*, 2020, **298**, 505–518.
- 43 C. A. Dreiss, *Curr. Opin. Colloid Interface Sci.*, 2020, **48**, 1–17.
- 44 S. Bernhard and M. W. Tibbitt, *Adv. Drug Delivery Rev.*, 2021, **171**, 240–256.
- 45 D. Keskin, G. Zu, A. M. Forson, L. Tromp, J. Sjollema and P. van Rijn, *Bioact. Mater.*, 2021, **6**, 3634–3657.
- 46 M. Nöth, E. Gau, F. Jung, M. D. Davari, I. El-Awaad, A. Pich and U. Schwaneberg, *Green Chem.*, 2020, **22**, 8183–8209.
- 47 A. C. Daly, L. Riley, T. Segura and J. A. Burdick, *Nat. Rev. Mater.*, 2020, **5**, 20–43.
- 48 D. J. McClements, *Adv. Colloid Interface Sci.*, 2017, **240**, 31–59.
- 49 H. M. Shewan and J. R. Stokes, *J. Food Eng.*, 2013, **119**, 781–792.
- 50 C. D. V. D. Kuckling, H.-J. P. Adler, A. Volkel and H. Colfen, *Macromolecules*, 2006, **39**, 1585–1591.
- 51 M.-R. Sung, H. Xiao, E. A. Decker and D. J. McClements, *J. Food Eng.*, 2015, **155**, 16–21.
- 52 S. M. Desmarais, H. P. Haagsman and A. E. Barron, *Electrophoresis*, 2012, **33**, 2639–2649.
- 53 M. Bjornmalm, Y. Yan and F. Caruso, *J. Controlled Release*, 2014, **190**, 139–149.
- 54 G. Prakash, A. Shokr, N. Willemsen, S. M. Bashir, S. R. Shin and S. Hassan, *Adv. Drug Delivery Rev.*, 2022, **184**, 114197.
- 55 S. Bazban-Shotorbani, E. Dashtimoghadam, A. Karkhaneh, M. M. Hasani-Sadrabadi and K. I. Jacob, *Langmuir*, 2016, **32**, 4996–5003.
- 56 S. Utech, R. Prodanovic, A. S. Mao, R. Ostafe, D. J. Mooney and D. A. Weitz, *Adv. Healthcare Mater.*, 2015, **4**, 1628–1633.
- 57 A. G. Hati, T. R. Szymborski, M. Steinacher and E. Amstad, *Lab Chip*, 2018, **18**, 648–654.
- 58 J. Koh, D. R. Griffin, M. M. Archang, A. C. Feng, T. Horn, M. Margolis, D. Zalazar, T. Segura, P. O. Scumpia and D. Di Carlo, *Small*, 2019, **15**, 35.
- 59 S. Yadavali, H. H. Jeong, D. Lee and D. Issadore, *Nat. Commun.*, 2018, **9**, 1222.
- 60 T. J. Merkel, K. P. Herlihy, J. Nunes, R. M. Orgel, J. P. Rolland and J. M. DeSimone, *Langmuir*, 2010, **26**, 13086–13096.
- 61 H. Z. Stanislav Dubinsky, Z. Nie, I. Gourevich, D. Voicu, M. Deetz and E. Kumacheva, *Macromolecules*, 2008, **41**, 3555–3561.
- 62 M. E. Helgeson, S. C. Chapin and P. S. Doyle, *Curr. Opin. Colloid Interface Sci.*, 2011, **16**, 106–117.
- 63 C. Qiu, M. Chen, H. Yan and H. Wu, *Adv. Mater.*, 2007, **19**, 1603–1607.
- 64 A. Harada, Y. Takashima and M. Nakahata, *Acc. Chem. Res.*, 2014, **47**, 2128–2140.
- 65 E. A. Appel, M. W. Tibbitt, M. J. Webber, B. A. Mattix, O. Veiseh and R. Langer, *Nat. Commun.*, 2015, **6**, 6295.
- 66 N. G. Hădărugă, G. N. Bandur, I. David and D. I. Hădărugă, *Environ. Chem. Lett.*, 2018, **17**, 349–373.
- 67 D. Harries, D. C. Rau and V. A. Parsegian, *J. Am. Chem. Soc.*, 2005, **127**, 2184–2190.
- 68 E.-S. Kwak and E. A. Gomez, *Chromatographia*, 1996, **43**, 659–662.
- 69 W. C. Cromwell, K. Bystróm and M. R. Eftink, *J. Phys. Chem.*, 1985, **89**, 326–332.
- 70 A. Kasprzak, M. Koszytkowska-Stawinska, A. M. Nowicka, W. Buchowicz and M. Poplawska, *J. Org. Chem.*, 2019, **84**, 15900–15914.
- 71 V. Koliwoška, M. Gál, M. Hromadová, M. Valášek and L. Pospíšil, *J. Org. Chem.*, 2011, **696**, 1404–1408.
- 72 D. Granadero, J. Bordello, M. J. Pérez-Alvite, M. Novo and W. Al-Soufi, *Int. J. Mol. Sci.*, 2010, **11**, 173–188.
- 73 S. Xian and M. J. Webber, *J. Mater. Chem. B*, 2020, **8**, 9197–9211.
- 74 H. Yan, Q. Jiang, J. Wang, S. Cao, Y. Qiu, H. Wang, Y. Liao and X. Xie, *Polymer*, 2021, **221**, 123617.
- 75 A. E. Widener, M. Bhatta, T. E. Angelini and E. A. Phelps, *Biomater. Sci.*, 2021, **9**, 2480–2493.
- 76 X. Liu, L. Zhao, F. Liu, D. Astruc and H. Gu, *Coord. Chem. Rev.*, 2020, **419**, 213406.
- 77 W. Xu, Q. Song, J.-F. Xu, M. J. Serpe and X. Zhang, *ACS Appl. Mater. Interfaces*, 2017, **9**, 11368–11372.
- 78 H. H. Jeong, V. R. Yelleswarapu, S. Yadavali, D. Issadore and D. Lee, *Lab Chip*, 2015, **15**, 4387–4392.
- 79 C. B. Rodell, J. W. MacArthur, S. M. Dorsey, R. J. Wade, L. L. Wang, Y. J. Woo and J. A. Burdick, *Adv. Funct. Mater.*, 2015, **25**, 636–644.
- 80 S.-H. Jung, S. Schneider, F. Plamper and A. Pich, *Macromolecules*, 2020, **53**, 1043–1053.
- 81 P. Wang, Q. Yang, Z. Ye, C. Zhao and J. Yang, *Macromol. Chem. Phys.*, 2017, **218**, 1700280.
- 82 K. Marcisz, D. Jaglencic, M. Mackiewicz, J. Romanski and M. Karbarz, *Mater. Today Chem.*, 2022, **26**, 101151.
- 83 L. Peng, A. Feng, S. Liu, M. Huo, T. Fang, K. Wang, Y. Wei, X. Wang and J. Yuan, *ACS Appl. Mater. Interfaces*, 2016, **8**, 29203–29207.
- 84 D. Taura, S. Li, A. Hashidzume and A. Harada, *Macromolecules*, 2010, **43**, 1706–1713.
- 85 Y.-L. Lin, S. Zheng, C.-W. Chang, M.-J. Lee, Y.-F. Chen and J.-T. Chen, *Macromolecules*, 2022, **55**, 8940–8949.
- 86 K. Han, D. Go, D. Hoenders, A. J. C. Kuehne and A. Walther, *ACS Macro Lett.*, 2017, **6**, 310–314.
- 87 Y. Tang, P. Cao, W. Li, M. He, Z. Dai and Y. Xiong, *Polymer*, 2021, **220**, 123575.

- 88 Y. Liu, H. Yang, Z. Wang and X. Zhang, *Chem. – Asian J.*, 2013, **8**, 1626–1632.
- 89 A. C. B. J. Mohanty, W. M. Nau and H. Pal, *J. Phys. Chem. B*, 2006, **110**, 5133.
- 90 I. Ghosh and W. M. Nau, *Adv. Drug Delivery Rev.*, 2012, **64**, 764–783.
- 91 H. Zou, J. Liu, Y. Li, X. Li and X. Wang, *Small*, 2018, **14**, 1802234.
- 92 Q. Song, Y. Gao, J. F. Xu, B. Qin, M. J. Serpe and X. Zhang, *ACS Macro Lett.*, 2016, **5**, 1084–1088.
- 93 Y. Zheng, Z. Yu, R. M. Parker, Y. Wu, C. Abell and O. A. Scherman, *Nat. Commun.*, 2014, **5**, 5772.
- 94 J. Liu, C. S. Y. Tan, Z. Yu, N. Li, C. Abell and O. A. Scherman, *Adv. Mater.*, 2017, **29**, 1605325.
- 95 D. J. Whitaker, Z. Huang, B. W. Longbottom, R. L. Sala, G. Wu and O. A. Scherman, *Polym. Chem.*, 2021, **12**, 519–525.
- 96 H. He, X. Cao, H. Dong, T. Ma and G. F. Payne, *Adv. Funct. Mater.*, 2017, **27**, 1605665.
- 97 A. S. Caldwell, B. A. Aguado and K. S. Anseth, *Adv. Funct. Mater.*, 2020, **30**, 1907670.
- 98 J. Pan, X. Wen, M. Wang, J. Li, X. Li, A. Feng, L. Zhang and S. H. Thang, *Macromol. Rapid Commun.*, 2022, **43**, 2200239.
- 99 C. M. López and A. Pich, *Macromol. Rapid Commun.*, 2018, **39**, 1700808.
- 100 E. Izak-Nau, S. Braun, A. Pich and R. Göstl, *Adv. Sci.*, 2022, **9**, 2104004.
- 101 C. Molano-López, S. Braun, M. Kather, A. Töpel, G. van Wissen and A. Pich, *Macromol. Chem. Phys.*, 2022, **224**, 2200213.
- 102 J. Xue, W. Ji, S. Dong, Z. Zhang, J. Gao, P. Yang, J. Nie and B. Du, *Langmuir*, 2019, **35**, 16353–16365.
- 103 H. Ding, X. Liang, X. N. Zhang, Z. L. Wu, Z. Li and G. Sun, *Polymer*, 2019, **171**, 201–210.
- 104 J. Lee, E. J. Choi, I. Varga, P. M. Claesson, S. H. Yun and C. Song, *Polym. Chem.*, 2018, **9**, 1032–1039.
- 105 J. Es Sayed, C. Meyer, N. Sanson and P. Perrin, *ACS Macro Lett.*, 2020, **9**, 1040–1045.
- 106 J. Es Sayed, M. Khoonkari, M. Oggioni, P. Perrin, N. Sanson, M. Kamperman and M. K. Włodarczyk-Biegun, *Adv. Funct. Mater.*, 2022, **32**, 2207816.
- 107 J. Es Sayed, C. Lorthioir, P. Banet, P. Perrin and N. Sanson, *Angew. Chem., Int. Ed.*, 2020, **59**, 7042–7048.
- 108 J. Cautela, V. Lattanzi, L. K. Månsson, L. Galantini and J. J. Crassous, *Small*, 2018, **14**, 1803215.
- 109 L. Zhang, Z. Cao, T. Bai, L. Carr, J.-R. Ella-Menye, C. Irvin, B. D. Ratner and S. Jiang, *Nat. Biotechnol.*, 2013, **31**, 553–556.
- 110 P. Zhang, F. Sun, C. Tsao, S. Liu, P. Jain, A. Sinclair, H.-C. Hung, T. Bai, K. Wu and S. Jiang, *Proc. Natl. Acad. Sci. U. S. A.*, 2015, **112**, 12046–12051.
- 111 T. Bai, F. Sun, L. Zhang, A. Sinclair, S. Liu, J.-R. Ella-Menye, Y. Zheng and S. Jiang, *Angew. Chem., Int. Ed.*, 2014, **53**, 12729–12734.
- 112 A. Sinclair, M. B. O'Kelly, T. Bai, H.-C. Hung, P. Jain and S. Jiang, *Adv. Mater.*, 2018, **30**, 1803087.
- 113 Z. Fu, L. Ouyang, R. Xu, Y. Yang and W. Sun, *Mater. Today*, 2022, **52**, 112–132.
- 114 D. Chimene, R. Kaunas and A. K. Gaharwar, *Adv. Mater.*, 2020, **32**, 1902026.
- 115 M. Dong, Y. Han, X. P. Hao, H. C. Yu, J. Yin, M. Du, Q. Zheng and Z. L. Wu, *Adv. Mater.*, 2022, **34**, 2204333.
- 116 B. Zhang, H. Li, J. Cheng, H. Ye, A. H. Sakhaei, C. Yuan, P. Rao, Y. F. Zhang, Z. Chen, R. Wang, X. He, J. Liu, R. Xiao, S. Qu and Q. Ge, *Adv. Mater.*, 2021, **33**, 2101298.
- 117 X. Peng, T. Liu, Q. Zhang, C. Shang, Q.-W. Bai and H. Wang, *Adv. Funct. Mater.*, 2017, **27**, 1701962.
- 118 K. Zub, S. Hoepfener and U. S. Schubert, *Adv. Mater.*, 2022, **34**, 2105015.
- 119 T. Birman and D. Seliktar, *Adv. Funct. Mater.*, 2021, **31**, 2100628.
- 120 L. Riley, L. Schirmer and T. Segura, *Curr. Opin. Biotechnol.*, 2019, **60**, 1–8.
- 121 P. S. Gungor-Ozkerim, I. Inci, Y. S. Zhang, A. Khademhosseini and M. R. Dokmeci, *Biomater. Sci.*, 2018, **6**, 915–946.
- 122 Q. Feng, D. Li, Q. Li, H. Li, Z. Wang, S. Zhu, Z. Lin, X. Cao and H. Dong, *ACS Appl. Mater. Interfaces*, 2022, **14**, 15653–15666.
- 123 M. Hirsch, A. Charlet and E. Amstad, *Adv. Funct. Mater.*, 2020, **31**, 2005929.
- 124 C. B. Highley, K. H. Song, A. C. Daly and J. A. Burdick, *Adv. Sci.*, 2019, **6**, 1801076.
- 125 M. Shin, K. H. Song, J. C. Burrell, D. K. Cullen and J. A. Burdick, *Adv. Sci.*, 2019, **6**, 1901229.
- 126 Y. Sun, Y. Q. You, W. B. Jiang, B. Wang, Q. Wu and K. Dai, *Sci. Adv.*, 2020, **6**, 1–10.
- 127 Y. Fang, Y. Guo, M. Ji, B. Li, Y. Guo, J. Zhu, T. Zhang and Z. Xiong, *Adv. Funct. Mater.*, 2021, **32**, 2109810.
- 128 S. P. Pasca, *Nature*, 2018, **553**, 437–445.
- 129 A. J. D. Kruger, O. Bakirman, L. P. B. Guerzoni, A. Jans, D. B. Gehlen, D. Rommel, T. Haraszti, A. J. C. Kuehne and L. De Laporte, *Adv. Mater.*, 2019, **31**, 1903668.
- 130 C. Colosi, S. R. Shin, V. Manoharan, S. Massa, M. Costantini, A. Barbetta, M. R. Dokmeci, M. Dentini and A. Khademhosseini, *Adv. Mater.*, 2016, **28**, 677–684.
- 131 I. T. Ozbolat and M. Hospodiuk, *Biomaterials*, 2016, **76**, 321–343.
- 132 Z.-T. Xie, D.-H. Kang and M. Matsusaki, *Soft Matter*, 2021, **17**, 8769–8785.
- 133 A. McCormack, C. B. Highley, N. R. Leslie and F. P. W. Melchels, *Trends Biotechnol.*, 2020, **38**, 584–593.
- 134 C. B. Highley, K. H. Song, A. C. Daly and J. A. Burdick, *Adv. Sci.*, 2019, **6**, 1801076.
- 135 D. L. Taylor and M. In Het Panhuis, *Adv. Mater.*, 2016, **28**, 9060–9093.
- 136 E. M. Ahmed, *J. Adv. Res.*, 2015, **6**, 105–121.
- 137 H.-R. Lin and K. C. Sung, *J. Controlled Release*, 2000, **69**, 379–388.
- 138 A. Lee, A. R. Hudson, D. J. Shiwerski, J. W. Tashman, T. J. Hinton, S. Yerneni, J. M. Bliley, P. G. Campbell and A. W. Feinberg, *Science*, 2019, **365**, 482–487.

- 139 J. M. Piau, *J. Non-Newtonian Fluid Mech.*, 2007, **144**, 1–29.
- 140 L. Ning, R. Mehta, C. Cao, A. Theus, M. Tomov, N. Zhu, E. R. Weeks, H. Bauser-Heaton and V. Serpooshan, *ACS Appl. Mater. Interfaces*, 2020, **12**, 44563–44577.
- 141 Y. Jin, A. Compaan, T. Bhattacharjee and Y. Huang, *Biofabrication*, 2016, **8**, 025016.
- 142 M. Z. Steven, B. Tapomoy, G. R. Kyle, S. Jain, M. N. Ryan, W. G. Sawyer and E. A. Thomas, *Sci. Adv.*, 2015, **1**, 1500655.
- 143 J. Y. Sun, X. Zhao, W. R. Illeperuma, O. Chaudhuri, K. H. Oh, D. J. Mooney, J. J. Vlassak and Z. Suo, *Nature*, 2012, **489**, 133–136.
- 144 O. Jeon, Y. B. Lee, H. Jeong, S. J. Lee, D. Wells and E. Alsberg, *Mater. Horiz.*, 2019, **6**, 1625–1631.
- 145 A. Shapira, N. Noor, H. Oved and T. Dvir, *Biomed. Mater.*, 2020, **15**, 045018.
- 146 M. H. Kim, D. Banerjee, N. Celik and I. T. Ozbolat, *Biofabrication*, 2022, **14**, 024103.
- 147 S. T. Koshy, R. M. Desai, P. Joly, J. Li, R. K. Bagrodia, S. A. Lewin, N. S. Joshi and D. J. Mooney, *Adv. Healthcare Mater.*, 2016, **5**, 541–547.
- 148 A. M. Compaan, K. Song, W. Chai and Y. Huang, *ACS Appl. Mater. Interfaces*, 2020, **12**, 7855–7868.
- 149 Y. Jiang, J. Chen, C. Deng, E. J. Suuronen and Z. Zhong, *Biomaterials*, 2014, **35**, 4969–4985.
- 150 L. Huang, A. M. E. Abdalla, L. Xiao and G. Yang, *Int. J. Mol. Sci.*, 2020, **21**, 1895.
- 151 F. Li, V. X. Truong, H. Thissen, J. E. Frith and J. S. Forsythe, *ACS Appl. Mater. Interfaces*, 2017, **9**, 8589–8601.
- 152 X. Zhao, S. Liu, L. Yildirimer, H. Zhao, R. Ding, H. Wang, W. Cui and D. Weitz, *Adv. Funct. Mater.*, 2016, **26**, 2809–2819.
- 153 B. Li, L. Wang, F. Xu, X. Gang, U. Demirci, D. Wei, Y. Li, Y. Feng, D. Jia and Y. Zhou, *Acta Biomater.*, 2015, **22**, 59–69.
- 154 S. Selimovic, J. Oh, H. Bae, M. Dokmeci and A. Khademhosseini, *Polymers*, 2012, **4**, 1554.
- 155 Z. Zhao, Z. Wang, G. Li, Z. Cai, J. Wu, L. Wang, L. Deng, M. Cai and W. Cui, *Adv. Funct. Mater.*, 2021, **31**, 2103339.
- 156 Y. Li, P. Chen, Y. Wang, S. Yan, X. Feng, W. Du, S. A. Koehler, U. Demirci and B.-F. Liu, *Adv. Mater.*, 2016, **28**, 3543–3548.
- 157 A. S. Mao, J. W. Shin, S. Utech, H. Wang, O. Uzun, W. Li, M. Cooper, Y. Hu, L. Zhang, D. A. Weitz and D. J. Mooney, *Nat. Mater.*, 2017, **16**, 236–243.
- 158 J. K. Oh, R. Drumright, D. J. Siegwart and K. Matyjaszewski, *Prog. Polym. Sci.*, 2008, **33**, 448–477.
- 159 D. Sivakumaran, D. Maitland and T. Hoare, *Biomacromolecules*, 2011, **12**, 4112–4120.
- 160 F. Topuz and T. Uyar, *Carbohydr. Polym.*, 2022, **297**, 120033.
- 161 Q. Qian, L. Shi, X. Gao, Y. Ma, J. Yang, Z. Zhang, J. Qian and X. Zhu, *Small*, 2019, **15**, 1903208.
- 162 X. Si, S. Ma, Y. Xu, D. Zhang, N. Shen, H. Yu, Y. Zhang, W. Song, Z. Tang and X. Chen, *J. Controlled Release*, 2020, **320**, 83–95.
- 163 Q. Song, Y. Yin, L. Shang, T. Wu, D. Zhang, M. Kong, Y. Zhao, Y. He, S. Tan, Y. Guo and Z. Zhang, *Nano Lett.*, 2017, **17**, 6366–6375.
- 164 I. Antoniuk, D. Kaczmarek, A. Kardos, I. Varga and C. Amiel, *Polymers*, 2018, **10**, 566.
- 165 X. Ding, A. Wang, W. Tong and F.-J. Xu, *Small*, 2019, **15**, 1900999.
- 166 F. Bures, *Top. Curr. Chem.*, 2019, **377**, 14.
- 167 S. Mohapatra, L. Yutao, S. G. Goh, C. Ng, Y. Luhua, N. H. Tran and K. Y. Gin, *J. Hazard. Mater.*, 2023, **445**, 130393.
- 168 M. Lei, A. Jayaraman, J. A. Van Deventer and K. Lee, *Annu. Rev. Biomed. Eng.*, 2021, **23**, 339–357.
- 169 L. J. Zhang and R. L. Gallo, *Curr. Biol.*, 2016, **26**, R14–19.
- 170 R. Nordstrom and M. Malmsten, *Adv. Colloid Interface Sci.*, 2017, **242**, 17–34.
- 171 B. Thallinger, E. N. Prasetyo, G. S. Nyanhongo and G. M. Guebitz, *Biotechnol. J.*, 2013, **8**, 97–109.
- 172 Q. Zhou, Z. Si, K. Wang, K. Li, W. Hong, Y. Zhang and P. Li, *J. Controlled Release*, 2022, **352**, 507–526.
- 173 B. C. Borro, R. Nordström and M. Malmsten, *Colloids Surf., B*, 2020, **187**, 110835.
- 174 Q. Wang, E. Uzunoglu, Y. Wu and M. Libera, *ACS Appl. Mater. Interfaces*, 2012, **4**, 2498–2506.
- 175 G. Zu, M. Steinmüller, D. Keskin, H. C. van der Mei, O. Mergel and P. van Rijn, *ACS Appl. Polym. Mater.*, 2020, **2**, 5779–5789.
- 176 Y. Wang, Y. Yang, Y. Shi, H. Song and C. Yu, *Adv. Mater.*, 2020, **32**, 1904106.
- 177 Z. Zhao, X. Ma, R. Chen, H. Xue, J. Lei, H. Du, Z. Zhang and H. Chen, *ACS Appl. Mater. Interfaces*, 2020, **12**, 19268–19276.
- 178 H. Xue, Z. Zhao, S. Chen, H. Du, R. Chen, J. L. Brash and H. Chen, *Colloid Interface Sci. Commun.*, 2020, **37**, 100268.
- 179 S. Panja, R. Bharti, G. Dey, N. A. Lynd and S. Chattopadhyay, *ACS Appl. Mater. Interfaces*, 2019, **11**, 33599–33611.
- 180 L. Moroni, J. A. Burdick, C. Highley, S. J. Lee, Y. Morimoto, S. Takeuchi and J. J. Yoo, *Nat. Rev. Mater.*, 2018, **3**, 21–37.
- 181 A. K. Gaharwar, I. Singh and A. Khademhosseini, *Nat. Rev. Mater.*, 2020, **5**, 686–705.
- 182 M. Bhattacharjee, J. Coburn, M. Centola, S. Murab, A. Barbero, D. L. Kaplan, I. Martin and S. Ghosh, *Adv. Drug Delivery Rev.*, 2015, **84**, 107–122.
- 183 R. D. Pedde, B. Mirani, A. Navaei, T. Styan, S. Wong, M. Mehrli, A. Thakur, N. K. Mohtaram, A. Bayati, A. Dolatshahi-Pirouz, M. Nikkhah, S. M. Willerth and M. Akbari, *Adv. Mater.*, 2017, **29**, 1606061.
- 184 A. Atala, *Chem. Rev.*, 2020, **120**, 10545–10546.
- 185 K. Zhang, Z. Jia, B. Yang, Q. Feng, X. Xu, W. Yuan, X. Li, X. Chen, L. Duan, D. Wang and L. Bian, *Adv. Sci.*, 2018, **5**, 1800875.
- 186 Q. Feng, H. Gao, H. Wen, H. Huang, Q. Li, M. Liang, Y. Liu, H. Dong and X. Cao, *Acta Biomater.*, 2020, **113**, 393–406.
- 187 Q. Feng, D. Li, Q. Li, S. Li, H. Huang, H. Li, H. Dong and X. Cao, *Adv. Healthcare Mater.*, 2022, **11**, 2102395.
- 188 F. Li, V. X. Truong, P. Fisch, C. Levinson, V. Glattauer, M. Zenobi-Wong, H. Thissen, J. S. Forsythe and J. E. Frith, *Acta Biomater.*, 2018, **77**, 48–62.
- 189 R. Madonna, L. W. Van Laake, H. E. Botker, S. M. Davidson, R. De Caterina, F. B. Engel, T. Eschenhagen,

- F. Fernandez-Aviles, D. J. Hausenloy, J. S. Hulot, S. Lecour, J. Leor, P. Menasche, M. Pesce, C. Perrino, F. Prunier, S. Van Linthout, K. Ytrehus, W. H. Zimmermann, P. Ferdinandy and J. P. G. Sluijter, *Cardiovasc. Res.*, 2019, **115**, 488–500.
- 190 H. N. Yang, J. H. Choi, J. S. Park, S. Y. Jeon, K. D. Park and K. H. Park, *Biomaterials*, 2014, **35**, 4716–4728.
- 191 R. Kumar, K. R. Aadil, S. Ranjan and V. B. Kumar, *J. Drug Delivery Sci. Technol.*, 2020, **57**, 101617.
- 192 R. S. Hsu, P. Y. Chen, J. H. Fang, Y. Y. Chen, C. W. Chang, Y. J. Lu and S. H. Hu, *Adv. Sci.*, 2019, **6**, 1900520.
- 193 X. Zhao, L. Jin, Z. Zhu, H. Lu, H. Shi, Q. Zhong, J. M. Oliveira, R. L. Reis, C. Gao and Z. Mao, *Appl. Mater. Today*, 2021, **23**, 101064.
- 194 T. J. Hinton, Q. Jallerat, R. N. Palchesko, J. H. Park, M. S. Grodzicki, H.-J. Shue, M. H. Ramadan, A. R. Hudson and A. W. Feinberg, *Sci. Adv.*, 2015, **1**, 1500758.
- 195 K. Ali, L. Robert, B. Jeffrey and P. V. Joseph, *Proc. Natl. Acad. Sci. U. S. A.*, 2006, **103**, 2480–2487.
- 196 J. L. Drury and D. J. Mooney, *Biomaterials*, 2003, **24**, 4337–4351.
- 197 P. M. Alison and M. V. Sefton, *Proc. Natl. Acad. Sci. U. S. A.*, 2006, **103**, 11461–11466.
- 198 C. Frantz, K. M. Stewart and V. M. Weaver, *J. Cell Sci.*, 2010, **123**, 4195–4200.
- 199 K. Pusch, T. J. Hinton and A. W. Feinberg, *HardwareX*, 2018, **3**, 49–61.
- 200 O. Jeon, Y. Bin Lee, T. J. Hinton, A. W. Feinberg and E. Alsberg, *Mater. Today Chem.*, 2019, **12**, 61–70.